MONGOLIAN PHYSICAL SOCIETY

ISSN 2414-9756

MONGOLIAN JOURNAL OF PHYSICS

SUPPLEMENT 2, SEPTEMBER 2020

Published by Mongolian Physical Society

9th International Conference on Materials Science

(ICMS2020)

September 10-13, 2020

Abstracts

Edited by Dr. N. Tuvjargal, Prof. J.Davaasambuu

Department of Physics, Faculty of Arts and Sciences,

National University of Mongolia

Ulaanbaatar

2020

DDC

015

X-71

Mongolian Journal of Physics. Supplement 2 presents the complete Abstracts of all contributions of the 9th International Conference on Materials Science (ICMS2020) in the National University of Mongolia, Ulaanbaatar, Mongolia, 10 -13 September 2020.

Published by the NUM Press, Ulaanbaatar, Mongolia

Ikh Surguuliin Gudamj – 1, Sukhbaatar District,

Ulaanbaatar – 14200, Mongolia

ISBN 978-99973-55-42-3

Preface

Dear colleagues,

We are pleased to welcome you to the 9th International Conference on Materials Science (ICMS2020) which will be held at the National University of Mongolia from 10th to 13th September 2020 in Ulaanbaatar.

The objectives of the conference are to bring together scientists working in the field of materials science from around the world, to exchange ideas, recent research results in this area and to offer a platform for the initiation of scientific cooperation between Mongolian and foreign scientists.

The conference will focus on the structures, properties and applications of new materials as well as their characterization techniques.

We would like to express our gratitude to all sponsors for their support in the realization of this conference and to the authors for submitting their abstracts to the ICMS2020.

On behalf of the Scientific Committee

Prof. Dr. Jav Davaasambuu

CONFERENCE ORGANIZERS

- Mongolian Physical Society, Mongolia
- National University of Mongolia, Mongolia
- Inner Mongolia Normal University, China
- Institute of Physical Materials Science, Siberian Branch of the Russian Academy of Sciences, Russia
- Buryat State University, Russia
- Mongolian Academy of Sciences, Mongolia
- German-Mongolian Institute for Resources and Technology, Mongolia
- Margad Institute, Mongolia

CONFERENCE SPONSORS

- Mongolian Physical Society, Mongolia
- National University of Mongolia, Mongolia
- German-Mongolian Institute for Resources and Technology, Mongolia
- Inter science LLC, Mongolia

CONFERENCE COMMITTEES

Scientific committee:

- Prof. J.Davaasambuu (National University of Mongolia, Mongolia)
- Prof. U.Pietsch (University of Siegen, Germany)
- Prof. G.Eckold (University of Goettingen, Germany)
- Prof. B.Narsu (Inner Mongolia Normal University, China)
- Prof. O.Tegus (Inner Mongolia Normal University, China)
- Prof. A.Nomoev (Institute of Physical Materials Science, Siberian Branch of the Russian Academy of Sciences,Russia)
- Prof. S.Gorfman (Tel Aviv University, Israel)
- Prof. S.Bardakhanov (Institute of Theoretical and Applied Mechanics SB RAS, Russia)
- Prof. P.Daniel (Le-Mans University, France)
- Prof. B.Battsengel (GMIT, Mongolia)
- Prof. B.B.Damdinov (Siberian Federal University, Krasnoyarsk, Russia)
- Acad. O.Penyazkov (A.V.Lykov Institute, Belarus)
- Acad. D.Sangaa (Mongolian Academy of Sciences, Mongolia)
- Acad. J.Temuujin (Mongolian Academy of Sciences, Mongolia)
- Prof. G.Shilagardi (National University of Mongolia, Mongolia)
- Dr. V.Koledov (IRE, RAS, Russia)
- Dr. P.Altantsog (Mongolian Academy of Sciences, Mongolia)

Organizing committee:

- Dr. N.Tuvjargal (National University of Mongolia)
- Prof. Ts.Amartaivan (National University of Mongolia)
- Prof. D.Ulam-Orgikh (National University of Mongolia)
- Dr. E.Uyanga (Mongolian Academy of Sciences)
- Dr. Ts.Enkhbat (Mongolian Physical Society)
- Prof. L.Enkhtur (National University of Mongolia)
- Prof. J.Vanchinkhuu (National University of Mongolia)
- Prof. N.Tsogbadrakh (National University of Mongolia)
- Dr. S.Munkhtsetseg (National University of Mongolia)
- Dr. G.Erdene-Ochir (National University of Mongolia)
- Prof. Altan Bolag (Inner Mongolia Nornal University, China)
- Dr. Vyacheslav Syzrantsev (Institute of Physical Material Science of SB RAS, Russia)
- Dr. Tsetsenbaatar (Inner Mongolia Nornal University, China)
- Dr. Ch.Aldarmaa (MUST, Mongolia)
- Dr. G.Munkhbayar (National University of Mongolia)
- Dr. Ts.Erdenechuluun (Margad Institute, Mongolia)

Scientific Program:

11 September (Friday) (# 502 room of NUM library)

09.00-10.00	Registration (Coffee break)
10.00-10.30	Opening Prof. Dr. J.Davaasambuu (President of Mongolian Physical Society, Mongolia) Prof. Dr. Andrey Nomoev (Institute of Physical Material Science SB RAS, Russia) Prof. Dr. Bai Narsu (Inner Mongolia Normal University, China)
Chairman: Prof. R.Galbadrakh (National University of Mongolia)	
10.30-11.00	**Keynote lecture by Acad. J.Temuujin** (Mongolian Academy of Sciences) ***The latest development of coal combustion by-products utilization research in Mongolia***
11.00-11.15	**Some results of ferrite magnetic nano materials research** *D.Sangaa, N.Jargalan, I.Khishigdemberel, B.Enkhmend, E.Uyanga, T.Yu.Kiseleva*
11.15-11.30	**Scanning tunneling microscopy observation of WSe_2 surface morphology deposited on SiO_2/Si surface** *G. Munkhsaikhan, D.Otgonbayar, B. Odontuya, D. Naranchimeg, R.Buyanjargal*
11.30-11.45	**Study of Copper Doped Zinc oxide Nanoparticles** *Ariunzaya Tsogoo, Erdene-Ochir Ganbold, Ninjbadgar Tsedev, Philippe Daniel, Alain Gibaud, Nomin-Erdene Battulga, Bayasgalan Ulambayar, Rentsenmyadag Dashzeveg*
11.45-12.00	**Design and construction of a mirror-dispersion-controlled Ti:sapphire oscillator** *D.Unurbileg, Ts.Khos-Ochir, E.Nomin-Erdene, P.Munkbaatar, J.Davaasambuu*

12.00-14.00	Lunch
Chair persons: Prof. Dr. Vyacheslav Syzrantsev (Institute of Physical Material Science of SB RAS, Russia) Dr. Ch.Aldarmaa (Mongolian University of Science and Technology)	
14.00-14.30	**Keynote lecture by Dr. Svetlana von Gratowski** (Institute of Radio Engineering and Electronics, Russian Academy of Sciences, Russia) ***Mechanical bottom-up nano-assembling and nano-manipulation using shape memory alloy nano-gripper***
14.30-14.45	**Polyethylene terephthalate filaments with glycol and carbon microfibers** *A.V.Nomoev, V.V.Syzrantsev, U.L.Mishigdorzhiyn, E.Ch.Khartaeva, V.N.Mankhirov, V.V.Lygdenov*
14.45-15.00	**T-x-y-z diagram prediction for the quaternary system Li,Na,Ca,La||F** *V. P. Vorob'eva, A. E. Zelenaya, V. I. Lutsyk, M. V. Lamueva*
15.00-15.15	**Material balances design in the $YbAl_2$-Al-$SrYb_4$ subsystem** *M. D. Parfenova, A. E. Zelenaya, V. I. Lutsyk*
15.15-15.30	**Dynamic viscosity of dispersion of silica dioxide nanoparticles** *T.S.Dembelova, S.A.Balzhinov, D.N. Makarova, Ye.D.Vershinina, S.B. Bazarova and B.B. Badmaev*
15.30-15.45	**Thermodynamic aspects of electron-beam surface modification of low-carbon steel** *Undrakh Mishigdorzhiyn, Nikolay Ulakhanov, Aleksandr Milonov, Pavel Guliashinov, Alexander Semenov*
15.45-16.00	**Determination of nanoscale layer thickness adsorbed liquid by acoustoelectric methods** *I.G. Simakov, Ch. Zh. Gulgenov, S.B. Bazarova*

16.00-16.15	**Structural, surface and optical properties of nanoalumina produced by various ways** *V.V. Syzrantsev, T.V. Larina, Yu.A. Abzaev, E.A. Paukstis, A.I. Kostyukov*
16.15-16.30	**Terahertz photoconductive antenna with annealing ohmic contacts: modeling and experiment** *S.A. Nomoev, I.S. Vasilevskii, A.N. Vinichenko*
16.30-17.30	**Coffee break, Poster session**

12 September (Saturday) (# 502 room of NUM library)

Chair persons: Prof. Dr. Altan Bolag (Inner Mongolia Normal University) Prof. N.Tsogbadrakh (National University of Mongolia)	
09.00-09.30	**Keynote lecture by Dr. Victor Koledov** (Institute of Radio Engineering and Electronics, Russian Academy of Sciences, Russia) *New functional nano-materials for nanotechnology, biomedicine and energy*
09.30-9.45	**Hydrogen bonding interactions between ethylenedimine-functionalized protic ionic liquids having TF/ TFA/ hexanoylalaninate anions and carbon dioxide** *Huang Hui, Liu Zheng, Hua Er*
09.45-10.00	**Development of a Series of Novel Co-Sensitizers for Dye-Sensitized Solar Cells Based on N719** *Xin-Xin Wang, Altan Bolag, Wu Yun, Tana Bao, Jun Ning, Hexig Alata, Tegus Ojiyed*
10.00-10.15	**Modified Electronic Structure of Ta_2O_5 Via Surface Decorated with Ta_3B_2 Nanodots for Enhanced Photocatalytic Activity** *Lihong Bao, Fan Yang, Dawei Cheng, Xiaojian Pan, Hongyan Zhang, Fengqi Zhao, Siqin Zhao, O. Tegus*
10.15-10.30	**$Sc_{0.28}Ti_{0.72}Fe_{2-x}T_x$ alloys with T = Mn or Co: phase diagrams and magnetocaloric effect** *Sun-Liting, H. Yibole, O. Tegus and F. Guillou*
10.30-10.45	**Origin of Anisotropy in Gadolinium Crystal** *Dan Wei, Zhibin Chen, Hui Yang, Yongjun Cao, and Chuan Liu*
10.45-11.00	**Magnetic properties of flux grown $MnFe_4Si_3$ single crystal** *H. Yibole, W. Hanggai, Z.Q. Ou, O. Tegus, F. Guillou*

11.00-11.30	Coffee break
11.30-11.45	**Elastic theory for self-formed 3D nano-/micro- architectures** *Bai Narsu*
11.45-12.00	**Study on phase stabilization of black phosphorene** *Tana Bao, X. Tian, Narengerile, O.Tegus*
12.00-14.00	Lunch
Chairman: Prof. J.Vanchinkhuu (National University of Mongolia)	
14.00-14.15	**Study of order-disorder phase transitions in Cu-Au alloys using X-ray diffuse scattering** *L.Enkhtor, V.M.Silonov, Ts.Gantulga, Kh.Balt-Erdene, A.Badmaarag*
14.15-14.30	**$Li_4Ti_5O_{12}$/graphene composite as anode for li-ion batteries** *L.Sarantuya, N.Tsogbadrakh, A.Munkhbaatar, G.Sevjidsuren, P.Altantsog*
14.30-14.45	**Density functional calculation of excited states of atoms using CWDVR approach** *D.Naranchimeg, G.Munkhsaikhan[1], L.Khenmedekh, N.Tsogbadrakh, O.Sukh*
14.45-15.00	**Design of experiments in optimization of motor parameters** *Ariunbolor Purvee*
15.00-15.30	Coffee break
Chairman: Prof. L. Enkhtur (National University of Mongolia)	
15.30-15.45	**Preparation of porous material from Mongolian clay minerals** *G.Oyun-Erdene, D.Anudari, L.Mandakhsaikhan, Z.Zolzaya, J.Temuujin*

15.45-16.00	**Synthesis of Silver Nanoparticles by Hydrothermal Processing** *E.Surenjav, B. Buyankhishig, N. Byamba-Ochir, N. Davaadorj, S.Zhiqiang and O. Tegus*
16.00-16.15	**Metallic thickness optimization of a monometallic plasmonic structure for a surface-plasmon resonance biosensor** *E.Nomin-Erdene, Ts.Khos-Ochir, A.Nomin, B.Khishigsuren, B.Zaya, O.Oidovsambuu, G.Munkhbayar, J.Davaasambuu*
16.15-16.30	**Thermal coatings for tribologically highly loaded parts of pump** *Ariunbolor Purvee, Gunther C. STEHR, Battsengel Baatar*
16.30-16.45	**Improvement of imaging and image correction methods of soft X-ray projection microscopy** *B.Duurenbuyan, J.Erdenetogtokh, J.Vanchinkhuu, Tatsuo Shiina, Yasuhito Kinjo, Atsushi Ito*
16.45-17.00	**Discussion & Closing**

POSTER SESSION

P1. $Gd_3Al_4GaO_{12}:Cr^{3+}$ Phosphors for Far-Red Light Emitting Diodes

Xiang Li, Dahai Hu,Yizhi Ma, Xinran Wan, Fengxiang Wan, Zhiqiang Song, Qier Sa, Kefu Chao

P2. Bonding effects on the crystal structure, magnetic and mechanical properties of Fe_2P-based Mn-Fe-P-Si compound

Jiaying Zhang, Dan Zhao, Zhiqiang Ou

P3. Dynamic potential deposition of CuGa oxides

Linrui Zhang, Bingqing Zhou

P4. XRD and EXAFS Study on Preparation Process of the $Mn_{125}Fe_{70}P_{50}Si_{50}$ Compound

Yingjie Li , YuanjieHao, Zhiqiang Ou, O Tegus, Ikuo Nakai

P5. Solubility and aggregation behavior of alanine magnesium complexes

Naren Gerile, Yifeng Shi, Ying Zhang, Tana Bao, O. Tegus

P6. Structure and magnetocaloric effect of $Mn_{1.25}Fe_{0.75}P_{0.50}Si_{0.50}B_x$ alloys

Shouyuan Xing, Jiaying Zhang, Lin Song, and Zhiqiang Ou

P7. An Analysis of Some Bronzes Excavated from the Xindianzi Cemetery in Inner Mongolia

Song Zhiqiang, Sun Jinsong,Yong Mei,Cao Jianen, O Tegus

P8. Magnetostriction and microstructure of $Fe_{100-x}Al_x$ alloys

Rui Wang, Xiao Tian, Zhanquan Yao

P9. Preparation of the efficient Inverted Perovskite Solar cells with NiO as hole transport layer

Wenbing Meng, Yali Zhu, Xiaoyu Lv, Jun Ning, Alata Hexig, Bingqin Zhou, O.Tegus

P10. Effects of different polar groups on the Liquid Crystal properties of the yttrium (III) Acyl –Alaninate Complexes

Zhang Ying, Naren Gerile, Zhang Jinkang, Shi Yifeng, Alatan Bolag，O.Tegus

P11. Preparation and spectrial studies of silicon nitride thin films containing amorphous silicon quantum dots

Zhou Bingqing, Gu Xin, Sun Jiaxin

P12. Synthesis of nitrogen-doped hierarchical porous carbon materials and its catalytic ability in hydrogen evolution reaction

Li Jinhao, Zhang wunengerile, Wu Yun, Muschin Tegshi, Jia Jingchun, Bao Agula

P13. Magnetic Properties of $MnFe_{0.6}Ni_{0.4}Si_{1-x}Al_x$ Alloys

Nuendute, Ou Zhiqiang, H. Yibole, Siqin Bator, O.Tegus

P14. Receiving, Modeling of Formation, Properties of Composite Metal/Semiconductor Nanoparticles

A.V. Nomoev, N.V.Yumozhapova, E.Ch. Khartaeva

P15. Aggregations of Fullerenes (C_{60}) in Water and NMP: A Molecular Dynamic Study

M.Chagdarjav, N.Jargalan, B.Batgerel, B.Mijiddorj

P16. Biocompatibility of $Mg_{0.8}Ni_{0.2}Fe_2O_4$ ferrite nanoparticles evaluated by in vitro cytotoxicity assays using HeLa cells

I.Khishigdemberel, N.Nomin, Gantulga, E.Uyanga, B.Enkhmend, Ts.Oyunsuren, D.Sangaa

P17. Antioxidant activity of blueberry peel

B. Khongor, B. Davaasuren, R. Khoroljav, D. Naidan, J. Erdenetogtokh

P18. Study on catalytic activity of citrate-stabilized silver nanoparticles

Bayasgalan Ulambayar, Nomin-Erdene Battulga, Ikhbayar Batsukh, Khaliun Nomin-Erdene, Ninjbadgar Tsedev, Rentsenmyadag Dashzeveg, Galbadrakh Ragchaa, Erdene-Ochir Ganbold

P19. Synthesis of Fe_2Co/Al_2O_3 by the Pechini method for use as catalyst in CNT preparation

Enkhtur Sukhbaatar, Tsog-Ochir Tsendsuren, Galbadrakh Ragchaa, Bayasgalan Ulambayar, Nomin-Erdene Battulga, Rentsenmyadag Dashzeveg, Erdene-Ochir Ganbold

P20. Solubility of Baganuur coal in imidazolium based ionic liquid as ([Bmim]Cl) by FTIR spectroscopic study

S.Munkhtsetseg, G.Erdene-Ochir, R.Galbadrakh, S.Enkhtur, A.N.Oleshkevich, N. M. Lapchuk

P21. Mechanical and optical properties of fullerene contained polymers

E.M.Spilevski, S.A.Filatov, A.D.Zamkovets, G.Shilagardi, D.Ulam-Orgikh, S.Munkhtsetseg, P. Tuvshintur, D. Tumurbaatar

P22. Electrical properties of titanium-fullerene films

P.Tuvshintur, D.Ulam-Orgikh, M.Otgonbaatar, S.Munkhtsetseg, E.M.Shpilevsky, G.Shilagardi

P23. Results of research on discharge products

J.Vanchinkhuu, B.Duurenbuyan, M.Anand, E.Bayanjargal

P24. Dielectrophoretic force application in separating powder materials

J.Vanchinkhuu, J.Erdenetogtokh, B.Duurenbuyan, B.Anand

P25. Method for decreasing erosion of technical tools in a condition of dry and friction

Oidov Jamyan, Purevjal Bayasgalan

P26. Electrophysical properties of Janus-like silver nanoparticles

T.A. Chimytov, A.V. Nomoev

P27. Solid-State [2+2] Photodemirization of *trans*-Cinnamic Acid Derivatives: *trans*-4-(trifluorometyl)cinnamic acid

Chantsalnyam Bariashir, Nergui Uranbileg, Khongorzul Batchuluun, Jargalsaikhan Lkhasuren, Tuvjargal Norovsambuu and Davaasambuu Jav

The latest development of coal combustion by-products utilization research in Mongolia

Jadambaa Temuujin

Laboratory of Materials Science and Technology, Institute of Chemistry and Chemical Technology, Mongolian Academy of Sciences, Ulaanbaatar 51, Mongolia

e-mail: temuujin.mgl@gmail.com

Abstract: With its geological reserve of over 170 billion tons, coal is the most abundant source of energy in Mongolia. In Mongolia now has been operating six thermal power stations. Moreover, only in Ulaanbaatar city's over 210000 families live in the Ger district and use over 600000 tons of coal briquette. Three thermal power plants operating in Ulaanbaatar city burns about 5 million tons of coal, resulting in more than 500 thousand tons of coal combustion by-products per year in Ulaanbaatar city. In the world, coal ashes produced in thermal power plants, boilers, and single ovens pose serious environmental problems. The utilization of various types of waste is one of the factors determining the sustainability of cities. Therefore, the processing of wastes for re-use or disposal is a critical topic in waste management and materials research.

According to research data, the air and soil quality within the Mongolian capital city has reached a disastrous level. The main reasons for air pollution in Ulaanbaatar reported being coal-fired stoves of the Ger residential district, thermal power stations, small and medium-sized low-pressure furnaces, and motor vehicles. Here we discuss our latest results on the utilization of fly ash for preparation of cement added base layer of paved asphalt road, zeolites for removal of hazardous cations from the tannery water, glass ceramics, and briquette ash from the Ger district for preparation of an adsorbent.

Using coal ashes were prepared advanced materials such as glass-ceramics with the hardness of 6.35 GPa, zeolite A with Cr (III) removal capacity of 35.8 mg/g. With 20% fly ash into 5-8% cement containing a mixture of road base layer,

the compressive strength reached ~ 4MPa, i.e., within the standard limit. Using coal ashes from briquettes used for Ger district habitants prepared a new type of adsorbent material capable of removing various organic pollutants from tannery water. This ash also showed weak leaching character in water and acidic environment, which opens up an excellent opportunity to utilize.

Keywords: fly ash; glass ceramics; zeolite A; cement added base layer of paved road; briquette ash; adsorbent

Some results of ferrite magnetic nano materials research

D.Sangaa[1], N.Jargalan[1], I.Khishigdemberel[1], B.Enkhmend[1], E.Uyanga[1], T.Yu.Kiseleva[2],

[1]*Institute of Physics and Technology, Mongolian Academy of Sciences, Ulaanbaatar, 13330, Mongolia*

[2] *Faculty of Physics, Moscow State University, Moscow, 119991, Russia*

Abstract: In recent years, the study of the process of heat generation in the AC magnetic field of magnetic materials has attracted the attention of researchers in the fields of biology and medicine. The study of heat generation in terms of its structure, composition, magnetic properties, and size of crystallization is an important part of research in the field of physics [1-3].

This type of research has been conducted in the department of Materials Science of Institute of Physics and Technology for the last 5 years. During this period, the theoretical and experimental studies of the crystal and magnetic structures of magnesium and copper ferrite-containing materials were performed [4-7]. According to the results of the study, copper doped magnesium ferrite revealed a phase transition from the tetragonal to the cubic structure and it determined by neutron scattering method. At this value of the copper content ($Mg_{0.4}Cu_{0.6}Fe_2O_4$), the highest heat emission (~ 39ºC) was also observed [6]. In addition, the use of ferrite-type magnetic materials as mixtures to improve the properties of the materials for protection of biological objects from radiation is being studied [8].

In order to conduct a comparative study of the heat generation ability of the materials by changing the particle size and magnetic properties, we are studying ferrite materials that containing Ni, Al and Cr metals. The use of magnetic and non-magnetic doping elements makes it possible to convert ferrite compounds into other magnetic properties, such as ferro, ferri, and para, and to study their properties and correlations.

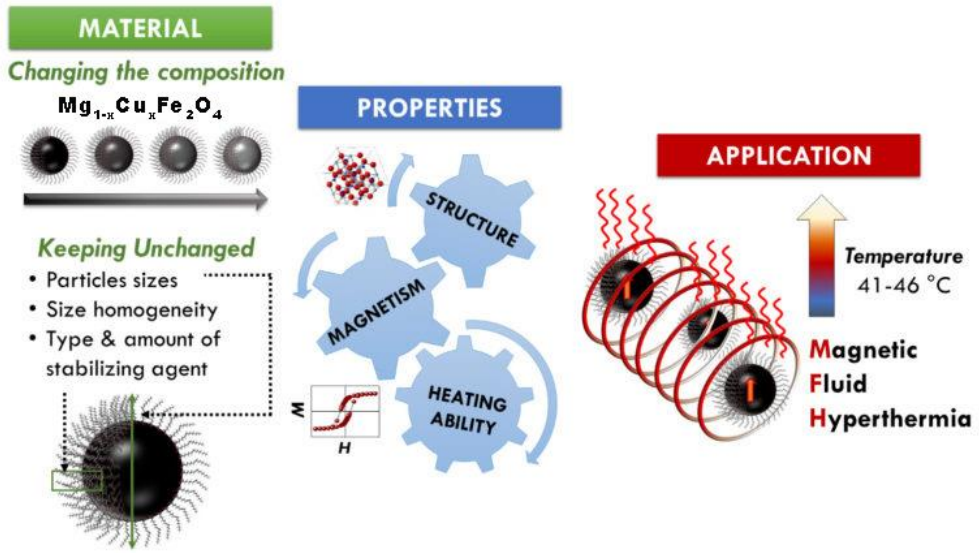

In this work, the experimental results of X-ray and neutron scattering, Mossbauer spectroscopy and theoretical calculation results for ferrite compounds with aluminum, chromium, copper and nickel doping elements and some experiments on cancer cell results are introduced.

References

[1]. W. Wu, Z. Wu, T. Yu, C. Jiang, W. Kim, Sci. Technol. Adv. Mater., 16, pp.161-3164, (2015).

[2]. H. Hirazawa, H. Aono, et al., J. Mag. Soc. Jap. 37, pp. 291-294, (2013).

[3]. M. Suto, Y. Hirota, H. Mamiya, A. Fujita, R. Kasuya, K. Tohji, B. Jeyadevan, J. Mag. Mag. Mat., 321, pp. 1493–1496, (2009).

[4]. H.Hirazawa, Y.Ito, D.Sangaa, N.Tsogbadrakh, H.Aono, T.Naohara "Heat generation ability in AC magnetic field of MgAlxFe2-xO4 ferrite powder prepared by sol-gel method" AIP Conference Proceedings 1763, 020009 (2016); doi: 10.1063/1.4961342

[5]. E. Uyanga, I. A. Bobrikov, D. Sangaa, H. Hirazawa, A. M. Balagurov. "Neutron diffraction study of crystal and magnetic structures of MgFe2O4 ferrite" Mongolian Journal of Physics, 2 (2016) 537–539.

[6]. I. Khishigdemberel, E. Uyanga, H. Hirazawa, D. Sangaa “Influence of Cu dope on the structural behavior of MgFe2O4 at various temperatures” Physica B: Condensed Matter, 544, (2018) 73–78

[7]. E. Uyanga, D. Sangaa, H. Hirazawa, N. Tsogbadrakh, N. Jargalan, I.A.Bobrikov, A.M. Balagurov. Structural investigation of chemically synthesized Ferrite magnetic nanomaterials. Journal of Molecular Structure 1160 (2018) 447–454.

[8]. Т. Ю. Киселева, Е. Т. Девяткина, Т. Ф. Григорьева, Е. В. Якута, Е. В. Лазарева, С. В. Восмериков, С. И. Жолудев, И. П. Иваненко, Г. П. Марков, Д. Сангаа, Е. Уянга, and А. С. Илюшин. Механосинтезированные композиционные материалы на основе сверхвысокомолекулярного полиэтилена, модифицированного частицами феррита магния. Физика и химия обработки материалов, 1, 57–68, 2020

Scanning tunneling microscopy observation of WSe_2 surface morphology deposited on SiO_2/Si surface

G. Munkhsaikhan, D.Otgonbayar, B. Odontuya, D. Naranchimeg, R.Buyanjargal

[1]*Department of Physics, School of Applied Sciences, Mongolian University of Science and Technology, Ulaanbaatar 14191, Mongolia.*

E-mail: gmunkhsaikhan@must.edu.mn

Abstract: In this work, the surface properties of the WSe_2 layers were studied using a scanning tunneling microscope (STM). A high-vacuum chamber exfoliation method is used to obtain a clean surface of WSe_2 samples with an atomic-sized smooth terrace or stepped layered structure. Two types of atomic defects have been revealed on the crystal structure and surface. These defects have been identified as the defects in the tungsten atom layer below the surface.

Keywords: Transition metal dichalcogenides, surface defects, topological surface, atomic terrace.

Study of Copper Doped Zinc oxide Nanoparticles

Ariunzaya Tsogoo[1, 2, a], Erdene-Ochir Ganbold[3], Ninjbadgar Tsedev[4], Philippe Daniel[1], Alain Gibaud[1], Nomin-Erdene Battulga[2], Bayasgalan Ulambayar[2], Rentsenmyadag Dashzeveg[2, b, *]

[1] *Institute of Molecules and Materials, Department of Physics, Le Mans University, 72000 Le Mans Cedex 9, France*

[2] *Department of Chemistry, School of Arts and Sciences, National University of Mongolia, University Street 1, Ulaanbaatar, 14201, Mongolia*

[3] *Department of Physics, School of Arts and Sciences, National University of Mongolia, University Street 1, Ulaanbaatar, 14201, Mongolia*

[4] *National University of Mongolia, University Street 1, Ulaanbaatar, 14201, Mongolia*

[a]*ariuka4@gmail.com*, [b]*d_rentsenmyadag@num.edu.mn*

Abstract: In this work transition metal copper (Cu) doped $Zn_{1-x}Cu_xO$ nanoparticles were synthesized by different doping concentration of Cu (x=1, 3, 5 and 7M%) through surfactant free benzyl alcohol route method in which zinc acetate, zinc acetylacetonate and copper acetate were selected as precursors. Crystal and structural analysis of all synthesized nanoparticles were determined by XRD and FT-IR. The XRD analysis demonstrated all reflection peaks with hexagonal wurtzite structure. The morphology and elemental analysis determined by TEM-EDX, TEM/STEM. Photocatalytic and antibacterial activity were studied by effectiveness of doping concentration. The methylene blue (MB) dye was used to investigate the photocatalytic experiment, 5m% Cu doped ZnO nanoparticles were showed high degradation efficiency. The antibacterial activity was tested in gram negative bacteria, *E. coli* and gram positive bacteria *S. Aureus* dilution method. After the doping significant antibacterial inhibition founded from 7M% Cu doped ZnO NPs for 98.9% and 97.4% for *E. coli* and *S. aureus*, respectively.

Keywords: Zinc oxide nanoparticles, Rhodamine 6G, photocatalytic activity, photo degradation, antibacterial activity, Escherichia Coli, Staphylococcus Aureus

Acknowledgements

This work is supported by the Asian Research Center Project (2018-3573).

Design and construction of a mirror-dispersion-controlled Ti: sapphire oscillator

D.Unurbileg[1], Ts.Khos-Ochir[1], E.Nomin-Erdene[1], P.Munkbaatar[1], J.Davaasambuu[1*]

[1] *Laser Research Center, National University of Mongolia*

P.O.Box 46A-390, 14201 Ulaanbaatar, Mongolia

*Corresponding author: [*davaasambuu@num.edu.mn](mailto:davaasambuu@num.edu.mn)*

Abstract: The motivation for generating ultra-short, intense, high quality optical pulses comes from many fields of physics and from other areas such as study of dynamics of chemical reactions or biological processes [1]. We will report on simplest cavity design of ultra-short Ti:sapphire oscillator which consists of only 5 elements: a gain medium – highly dopped Ti:sapphire crystal, a pair of GDD-oscillation compensated double chirped mirrors (DCM), a high reflectivity end mirror and output coupler. Due to thin gain medium, we had a chance of using only a pair of DCMs intra-cavity dispersion compensator going to produce 10 fs pulses with symmetric spectra [2]. Z folded linear cavity has round trip length of about 1.98 m which corresponds to repetition rate of 151 MHz. For our oscillator we estimated the proper folding angle at pump mirrors M2 and M3 as 15.22° to astigmatism compensation from Brewster cut of Ti: sapphire crystal [1][3]. As a pump laser, we use cw laser of 532 nm, Spectra-Physics Millenia-eV. The supporting mount of Ti: sapphire crystal is cooled to avoid heat accumulation and crystal temperature is measured by thermocouple was 19.5 – 19.9 °C under 3 W pumping energy.

Keywords: femtosecond laser, Ti: sapphire oscillator, dispersion compensation

This work was supported by Mongolian Foundation for Science and Technology, Fundamental Research Project Code Number: ШУСС2019/05

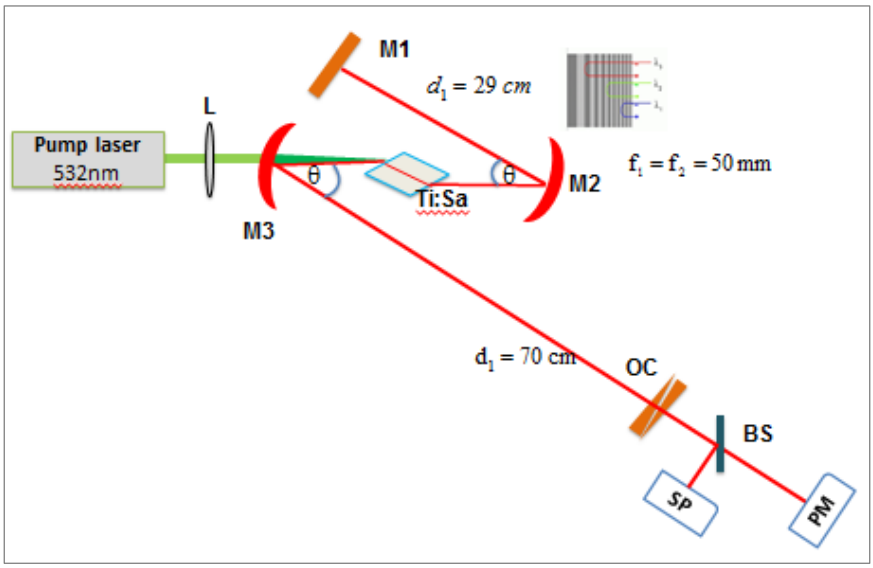

Fig. 1 Basic configuration of Ti:sapphire oscillator

Pump laser, Millenia@532 nm. L – focusing lens, M1 – high reflective mirror, Ti:sapphire – active medium, M2;M3 – pair of pump mirrors (DCM), OC- output coupler, BS –beam splitter, PM – powermeter

References

[1]. Shai Yefet and Avi Pe'er "A review of Cavity design for Kerr Lens Mode-Locked solid state lasers", *Appl.Sci.2013.3, 694-724; doi:10.3390/app3040694*

[1]. Robert S, Ferencz.K and Spielmann.C and Krausz.F, "Chirped multilayer coatings for broadband dispersion controlin femtosecond laser*", February 1, 1994 / Vol. 19, No. 3 / OPTICS LETTERS 201*

[2]. E.Nomin-Erdene, D.Unurbileg, P.Munkbaatar, Ts.Baatarchuluun, Ts.Khos-Ochir, G.Munkbayar, N.Tuvjargal, G.Erdene-Ochir, J.Davaasambuu, "Simulation of femtosecond pulse in a Kerr-lens mode locked Ti:sapphire laser", *IOP Conf. Ser.: Mater. Sci. Eng.* **704** 012008, doi:10.1088/1757-899X/704/1

Mechanical bottom-up nano-assembling and nano-manipulation using shape memory alloy nano-gripper

Svetlana von Gratowski

Institute of Radio Engineering and Electronics, Russian Academy of Sciences, Moscow part, Laboratory of magnetic materials, Mokhovaya 11-7, Moscow 125009, Russia

Abstract: The numerous nanoscale materials, such as nanoparticles and nanostructures in particular, 1-D and 2-D nanomaterials: nanotubes, nanowires (NWs), etc in the past decades were discovered and intensively studied. They had appeared to demonstrate the unique functional properties allowing construct the large number of individual nano-device based on individual nano-objects. Recently many studies have led to a broad range of proof-of-concept of individual nanoscale devices including nano-lasers, nano-sensors based on NWs and carbon nanotubes (CNT), field-effect transistors (nano-FETs), etc.

Such nano-devices represent attractive building blocks for hierarchical assembly. Hierarchical assembly of functional nanoscale/meso-scale and macroscopic devices from nanoscale building blocks based on individual nanoscale devices offers many opportunities for creating of micro- and –macro-devices and arrays by the bottom-up and hybrid paradigm. 5 steps in the bottom-up approach for production of nano-devices:1) to tailor (make) nanomaterials; 2) to etch (clean), passivate, or dope the surface of the nanomaterial; 3) to cut nanomaterials into individual components; 4) to fabricate elements and organize these elements or components into nano-devices. 5) to link (interconnect and integrate) individual nano-devices together into the micro,-meso- and -macro world. In the presentation proposed future application of the smallest and the fastest in the World nano-tweezer is able to manipulate real nano-objects like nanotubes, nanowires, etc.

Such nano-manipulation can be used for nano-manufacturing of nano-devices and micro-devices by mechanical nano-manipulation and bottom up

mechanical nano-assembling and nano-integration that in many cases can replaced very expensive with high running cost top-down nanolithography.

Polyethylene terephthalate filaments with glycol and carbon microfibers

A.V. Nomoev, V.V. Syzrantsev, U.L. Mishigdorzhiyn, E. Ch. Khartaeva, V.N.Mankhirov, V.V. Lygdenov

Institute of Physical Materials Science, Siberian Branch of the Russian Academy of Sciences, Sakhyanovoy st., 6, Ulan-Ude, 670047, Russia

e-mail: nomoevav@mail.ru

Abstract. Filaments of polyethylene terephthalate with glycol (PETG) with carbon microfibers promising for 3-D printing were obtained by extrusion; the structure was studied by scanning electron microscopy and elemental analysis was performed. In the process of manufacturing filaments, carbon microfibers are created and the possibility of changing the physical and mechanical properties - increasing the strength, melting temperature, due to the modification of PETG with carbon microfibers is shown.

References

[1]. A.V. Nomoev, D.S. Sanditov, V.V. Syzrantsev, B.R. Radnaev, M. Schreiber, Deformations of microindentations on glassy epoxy mixed with silica nanoparticles, Physica B: Condensed Matter (2019) 23-27.

[2]. https://innovax.info/oborudovanie-i-tehnologii/materialy/nylon-12cf-uglenapolnennyj/

[3]. D. Jiang and D.E. Smith. Mechanical behavior of carbon fiber composites produced with fused filament fabrication, Solid Freeform Fabrication 2016: Proceedings of the 27th Annual International Solid Freeform Fabrication Symposium – An Additive Manufacturing Conference Reviewed Paper .

[4]. http://www.bardakhanov.com/contact.html

T-x-y-z diagram prediction for the quaternary system Li,Na,Ca,La||F

V. P. Vorob'eva, A. E. Zelenaya, V. I. Lutsyk, M. V. Lamueva

Institute of Physical Materials Science, Siberian Branch of the Russian Academy of Sciences, Sakhyanovoy st., 6, Ulan-Ude, 670047, Russia

Abstract: The T-x-y-z diagram of the LiF-NaF-CaF2-LaF3 system has been predicted, based on the T-x-y diagrams 3D models of the boundary systems. 4D model of its prototype has been constructed. It includes three invariant transformations: the polymorphic transition between two modifications of calcium fluoride in the passive presence of liquid, LaF3 and the NaLaF4 compound, the quasi-peritectic and eutectic reactions. In general, the T-x-y-z diagram should consist of 169 hypersurfaces and 66 phase regions.

This work was been performed under the program of fundamental research SB RAS (project 0336-2019-0008), and it was partially supported by the RFBR projects 19-38-90035, 20-21-00056.

Material balances design in the $YbAl_2$-Al-$SrYb_4$ subsystem

M. D. Parfenova, A. E. Zelenaya, V. I. Lutsyk

Institute of Physical Materials Science, Siberian Branch of the Russian Academy of Sciences, Sakhyanovoy st., 6, Ulan-Ude, 670047, Russia

Abstract: The vertical mass balances - for the given center of masses, and the horizontal ones - for the isothermal state of isopleth, have been analyzed. These results are used for the different purposes: microstructures characterization, solidification paths confirmation, phase regions 3D-prototyping for the exploded diagram. It is once more showed, that a computer assembled model of the T-x-y diagram is a useful tool to solve different fundamental and applied tasks of the materials science.

This work was been performed under the program of fundamental research SB RAS (project 0336-2019-0008), and it was partially supported by the RFBR project 20-21-00056.

Dynamic viscosity of dispersion of silica dioxide nanoparticles

T.S. Dembelova[1*], S.A. Balzhinov[1], D.N. Makarova[1], Ye.D.Vershinina[1], S.B. Bazarova[1] and B.B. Badmaev[1]

[1]*Institute of Physical Materials Science of the Siberian Branch of the Russian Academy of Sciences, Ulan-Ude, 670047, Russia*

tu_dembel@mail.ru*

Abstract. Nanoscale objects significantly change the physical properties of both planar and bulk solid and liquid nanostructured systems. Nanoparticles as a dispersed phase lead to the appearance of a volumetric spatial structural network throughout the entire volume of the dispersed system. In this case, the structural and mechanical properties of the dispersed system change, and the relaxation processes occurring in them become more complicated. In this work, the dynamic viscosity of silica dioxide suspensions in polymer oils was investigated by acoustic, rotary and capillary methods. An installation has also been created for measuring the viscosity of a liquid at low gradients of the flow velocity, when one can expect that the structure of the liquid changes little during elementary acts of viscous flow. It is shown that at low flow rate gradients of the investigated suspensions, an increased (relative to the viscometric) value of viscosity is found, which indicates the structuring of these suspensions with the formation of a supramolecular structure. The observed phenomenon of increased viscosity can be of practical importance for all processes where slow flows prevail.

This work was partially supported by RFBR grant №18-48-030020 r_a.

Keywords: dispersion, nanoparticle, structure, liquid, polymer oil, viscosity, flow velocity gradient, viscometry.

Thermodynamic aspects of electron-beam surface modification of low-carbon steel

Undrakh Mishigdorzhiyn[1,2], Nikolay Ulakhanov[2],
Aleksandr Milonov[1], Pavel Guliashinov[3], Alexander Semenov[1]
[1]*Institute of Physical Materials Science SB RAS6 Sakhyanovoi, Str., 670047, Ulan-Ude, Russia*
[2]*East Siberia State University of Technology and Management, 40V Kluchevskaya, Str., 670013, Ulan-Ude, Russia*
[3]*Baikal Institute of Natural Management, SB RAS, 6 Sakhyanovoi, Str., 670047, Ulan-Ude, Russia*
druh@mail.ru

Abstract: Multicomponent surface modification of carbon steels is in high interest of mechanical engineering due to its valuable impact on surface properties of machine components and structures. The present research is devoted to possibility to simulate the process of aluminides and borides formation on the surface of low-carbon steel during electron beam alloying and predict the phase composition of obtained coatings. Computational thermodynamics and approximate calculation method are used to solve afore mentioned problem. Calculations are done in the temperature range 200 and 2000 K at 10^{-3} Pa. It was discovered that FeB and AlB_2 formation is possible on the steel surface.

Keywords: Electron beam surface modification, computational thermodynamics, low carbon steel, borides, aluminides

Determination of nanoscale layer thickness adsorbed liquid by acoustoelectric methods

I.G. Simakov, Ch. Zh. Gulgenov, S.B. Bazarova

Institute of Physical Materials Science, Siberian Branch of the Russian Academy of Sciences, Russia, 670047, Ulan-Ude, Sakhyanovoy st.6,

e-mail: baz_say@mail.ru

Abstract: It is shown to determine the thickness of the adsorbed liquid layer, it is proposed to use surface acoustic waves (SAW). The relative change in the SAW velocity is proportional to the thickness of the adsorption layer. The constant of proportionality is depending on the acoustic parameters of the solid (adsorbent) and the liquid in the layer. The velocity of sound in an adsorbed liquid depends on the thickness of the layer. For the determination of the velocity of sound in the liquid of the adsorption layer, it is proposed to use an original method based on comparing the parameters of bi-directional (differing in velocity) SAW.

Structural, surface and optical properties of nanoalumina produced by various ways

V.V. Syzrantsev[1(a)], T.V. Larina[2], Yu.A. Abzaev[3], E.A. Paukstis[2], A.I. Kostyukov[4]

[1] Institute of Materials Science of the Siberian Branch of the Russian Academy of Sciences, Ulan-Ude, Sakhyanovoy str. 6, 670070, Russia;

[2] Institute of Catalysis of the Siberian Branch of the Russian Academy of Sciences, Lavrentieva av. 5, Novosibirsk, 630090, Russia;

[3]Tomsk State University of Architecture and Building, Tomsk, Solyanaya sq. 2, 63400, Russia 3;

[4] Novosibirsk State University, Pirogova Str. 2, 630090, Novosibirsk, Russia;

[(A)]vvveliga@mail.ru

Abstract: The compared study of the properties of liquid-phase and electric explosion alumina nanoparticles was made. The X-ray diffraction analysis demonstrated that these nanoparticles remain in amorphous and semi-amorphous states. The complete structural information of Al_2O_3 nanoparticles was obtained as a result of the full-profile refinement of their model phase parameters. The parameters of the unit cells, spatial distribution of atoms, and occupancy of nodes were also determined.The data of IR spectra of surface OH groups and adsorbed CO revealed that the surface imperfection of an electric explosive sample is lower than that obtained using the liquid-phase method. Using photoluminescent spectroscopy, impurities of Cr^{3+}, Mn^{4+} and Ti^{3+} in the octahedral oxygen coordination and Fe^{3+} in the tetrahedral oxygen coordination were detected. It was observed that the concentration of these impurities was significantly higher in the electric explosion sample. Using UV-Vis DR spectroscopy, it was found that the liquid-phase sample was amorphous, and the electric explosive sample was well crystallized and most probably consisted of 2D and 3D nanostructures.

Terahertz photoconductive antenna with annealing ohmic contacts: modeling and experiment

S.A. Nomoev[1], I.S. Vasilevskii[1], A.N. Vinichenko[1]

[1]*National Research Nuclear University MEPhI (Moscow Engineering Physics Institute)*

Kashirskoe highway 31, Moscow, 115409, Russia

Email: serganom@gmail.com

Abstract: The area of the electromagnetic spectrum of terahertz (THz) radiation with wavelengths of approximately 0.1 to several millimeters is widely used: new devices are being intensively created to ensure life safety, medical diagnostics, non-destructive technological and operational control, due to the advantages of a harmless action on biological objects and a fairly high penetrating power, while maintaining high spatial resolution [1, 2].

The paper presents the results of numerical simulation of a terahertz (THz) photoconductive antenna with fired electrodes by the finite element method, Fig. 1. The simulation results indicate that the proposed THz antenna has a higher photocurrent than a conventional photoconductive antenna with annealing ohmic contacts. Higher THz power can potentially be obtained using the proposed photoconductive antenna with built-in electrodes. The simulation results show that the electric field strength on the surface is higher for conventional PCA, however, at the depth, the PCA with fired contacts has a higher electric field strength. The simulation results show that the increase in the photocurrent is directly proportional to the thickness of the fired contacts. The results of the performed experiments are consistent with the conclusions of the modeling.

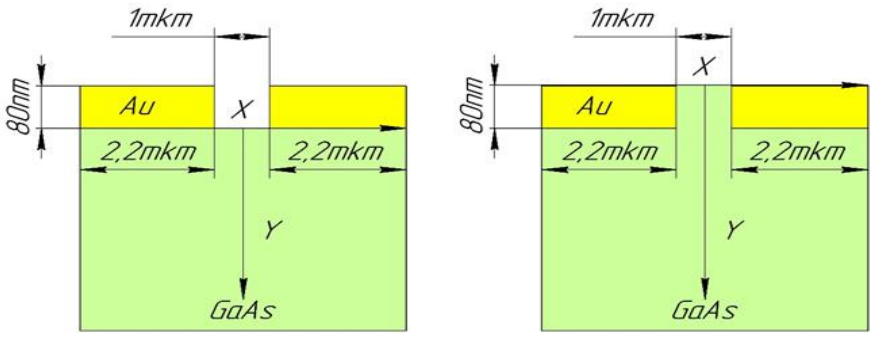

Fig.1. Schematic diagram of the structure of a photoconductive antenna; (a) - conventional model, (b) - with annealing ohmic contacts.

References

[1]. J. Baxter, G. Guglietta, Anal. Chem., **83**, 4342, (2011).

[2]. P. Jepsen, D. Cooke, M. Koch, Laser Photon, **5**, 124, (2011).

New functional nano-materials for nanotechnology, biomedicine and energy

Victor Koledov

Institute of Radio Engineering and Electronics, Russian Academy of Sciences, Moscow part, Laboratory of magnetic materials, Mokhovaya 11-7, Moscow 125009, Russia

Abstract: In recent decades new functional solid state materials have attracted much attention of material scientists, physicists and engineers. The physical basement of the unique functional properties of the new materials is often associated with phase transitions that manifest themselves in a solid state: magnetic, structural, superconducting ones. The resulting "giant" effects of the striking controlled change of size, shape, entropy, conductivity etc. in these materials under action of heating/cooling, stress and/or magnetic field exceed by the orders of magnitude the usual effects of magnetostriction, thermal expansion... These effects provide the new opportunities for next step engineering, microsystem technology, biomedical technology and alternative energy. Several new kinds of the solid state functional materials with phase transitions will be described in the lecture, including magnetic and nonmagnetic shape memory alloys, magnetocaloric materials based on Heusler alloys and rare Earth elements.

The devices based on them and their prospective applications will also be detailed. Particularly, the new technology of the composite shape memory mechanical nanotools with record small dimensions and high frequency of operation will be described. New room temperature applications of the magnetocaloric effect and magnetic functional materials for solid state refrigerators and heat pumps will be outlined. The new ideas of the economical high magnetic field generation for electrical engineering, super high speed vacuum magnetic levitating transportat and medical diagnostics will be discussed. The 10 years' experience of the new shape memory dental implant system based on nanostructural

shape memory materials for treatment of the patients with severe dental diseases will also be reported.

Hydrogen bonding interactions between ethylenedimine-functionalized protic ionic liquids having TF/ TFA/hexanoylalaninate anions and carbon dioxide

Huang Hui, Liu Zheng, Hua Er*

North Minzu University,Chemical Science and Engineering College

Email: huaer0101@hotmail.com

Abstract: Protic ionic liquids (PILs) composed of 2-ethylhexylethylenediaminium cation and trifluoromethanesulfonate (TFS), trifluoroacetate (TFA), hexanoylalaninate (Hexala) anions i.e. [HEtHex][TFS], [HEtHex][TFA], [HEtHex][Hexala] are expected to efficiently absorb CO_2 because of their having chelate-amine holes. Thus, the hydrogen bonding interaction between PILs and nCO_2 (n= 1, 2) molecules was investigated using the DFT theory at M06-2X/6-311G (*d*, *p*) level. The medium or weak O…H—N type hydrogen bonding is mainly formed between amine active site of cation and O atom of CO_2. The results of interaction energy, vibration spectra, stabilization energy, electron density show that the strength of hydrogen bonding interactions is in the order [HEtHex][TFS]-$n$$CO_2$>[HEtHex][TFA]-$n$$CO_2$> [HEtHex][Hexala]-$n$$CO_2$.

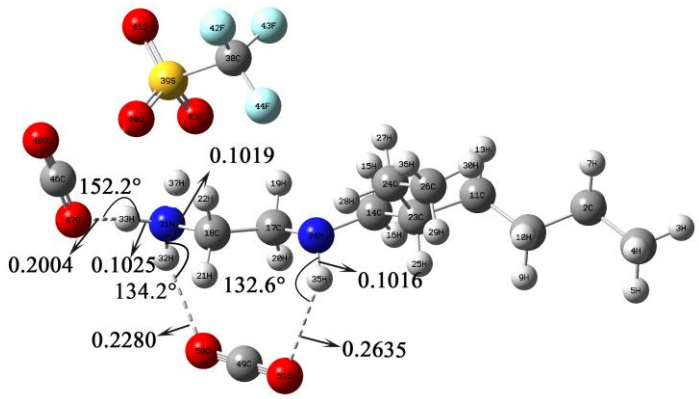

Fig.1 The optimized configuration of [HEtHex][TFS]-2CO_2, color code: blue N, gray C, red O, light blue F and light gray H

Furthermore, it has been revealed that the hydrogen bonding interactions between PILs and nCO$_2$ increase with increasing the amount of CO$_2$ molecules.

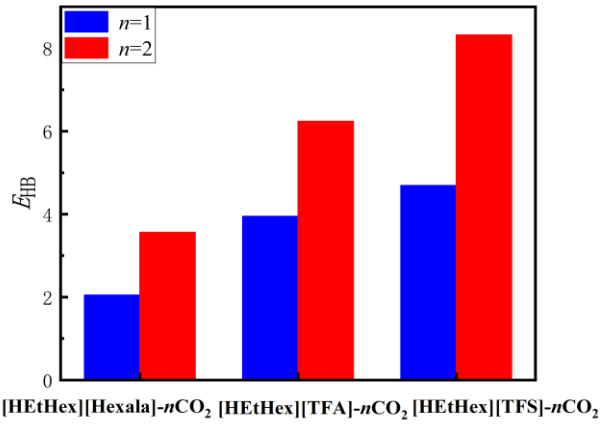

Fig.2 The hydrogen bonding energies (E_{HB} / kcal mol^{-1}) for PILs-nCO$_2$

References

[1]. [1] Y. Xu, Hua Er*, Hydrogen bonding study on protic ionic liquids composed of *N*-alkylethylenediaminum cations with trifluoroacetic anion, *Chemical Journal of Chinese Universities*, **39**(9), 1954-1960, 2018.

[2]. **H. Huang**, X. Zheng, Z. Liu, Hua Er*, H. Li*, Hydrogen bonding interactions between protic ionic liquids composed of 2-ethylhexylethylenediaminium cation and bis(trifluoromethanesulfonate)imide anion with water molecules, *Journal of Shihezi University (Natural Science)*, in press, 2020.

[3]. X. Zheng, Hua Er*, Hydrogen bonding interactions between protic ionic liquids composed of 2-ethylhexylethylenediaminium cation and trifluoroacetic/trifluoromethanesulfonate anions with water molecules, *Journal of Shihezi University (Natural Science)*, in press, 2020.

Development of a Series of Novel Co-Sensitizers for Dye-Sensitized Solar Cells Based on N719

Xin-Xin Wang[1,2], Altan Bolag[1]*, Wu Yun[2], Tana Bao[1], Jun Ning[1], Hexig Alata[1], Tegus Ojiyed[1]

[1] College of Physics and Electronic Information, Inner Mongolia Key Laboratory for Physics and Chemistry of Functional Materials, Inner Mongolia Normal University, Hohhot, 010020, China.

[2] College of Chemistry and Environmental Science, Inner Mongolia Key Laboratory for Environmental Chemistry, Inner Mongolia Normal University, Hohhot, 010020, China

Abstract: In the near decades, the research and application of dye-sensitized solar cells (DSC) received extensive attention in the field of science and technology. Typical ruthenium dyes (N719, N749, N3 and so on) used for DSCs usually absorb over a wide range of wavelength from 350 to 900 nm attributing to the metal-to-ligand charge-transfer (MLCT) transition. However, their molar extinction coefficients are relatively low as compared to pure organic sensitizers that possess intramolecular charge-transfer (ICT) in the same wavelength range. Based on this, utilization of joint ruthenium complexes and organic dyes for co-sensitizing metal oxide anode supposed to be a feasible tactic for complementing photo-absorption ability of DSSC. In this study, a series of novel symmetrical diphenylpyranylidene derivatives has been designed, prepared, characterized and studied for the application of DSC as a good co-sensitizer for enhancing the photovoltaic performance of ruthenium dye N719-based DSC.

This work was financially supported by the National Natural Science Foundation of China (21762033), High-level Funding Project of Ministry of Human Resources and Social Security of China, High-level Project of Inner Mongolia Normal University (2015YJRC001)

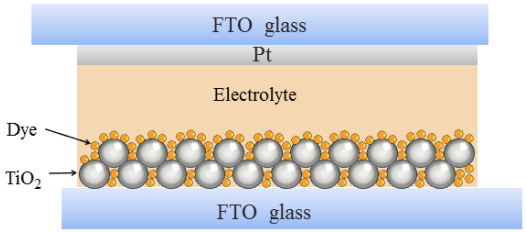

Fig. 1. Device structure of DSC

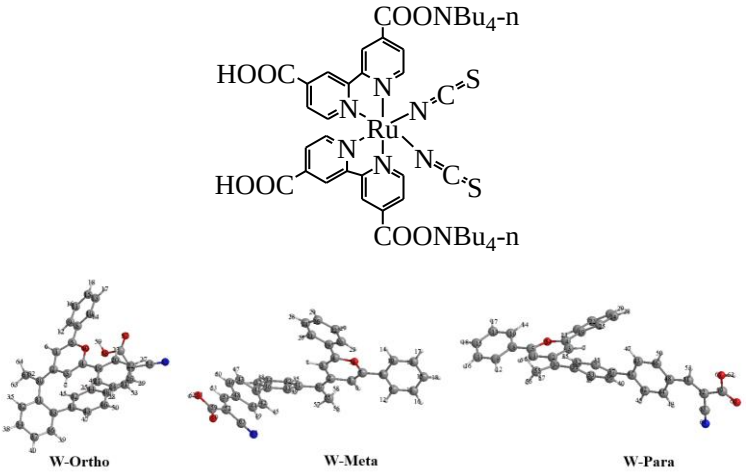

Fig. 2. Molecular Structure of N719 dye and calculated geometric structure of a series of co-sensitizers used for N719-based DSC.

References

[1]. M. Barrera, I. Crivelli, B. Loeb, *J Mol Model* **22**, 118, (2016).

[2]. S. Aghazada, M. K. Nazeeruddin, *Inorganics*, **6**, 52, (2018).

[3]. C. P. Woodward, T. Rüther, C. I. Coghlan, T. W. Jones, Y. Hebting, R. L. Cordiner, R. E. Dawson, D. E. J. E. Robinson, C. M. Forsyth, G. J. Wilson, *ChemPlusChem.*, **83**, 691, (2018).

[4]. J. Luo, Z. Wan, C. Jia, Y. Wang, X. Wu, X. Yao, *Electrochimica Acta*, **211**, 364, (2016).

[5]. D. D. Babu, R. Su, A. El-Shafei, A. V. Adhikari, *Electrochimica Acta*, **198**, 10, (2016).

Modified Electronic Structure of Ta_2O_5 Via Surface Decorated with Ta_3B_2 Nanodots for Enhanced Photocatalytic Activity

Lihong Bao[1,2], Fan Yang[2], Dawei Cheng[2], Xiaojian Pan[2], Hongyan Zhang[2], Fengqi Zhao[2], Siqin Zhao[3], O. Tegus[1]

[1]*Inner Mongolia Key Laboratory for Physics and Chemistry of Functional Materials, Inner Mongolia Normal University, Hohhot 010022, China*

[2]*College of physics and Electronic Information, Inner Mongolia Normal University, Hohhot 010022, China*

[3] *College of chemistry and Environmental Science, Inner Mongolia Normal University, Hohhot 010022, China*

Email: baolihong@imnu.edu.cn

Abstract: Metallic-semiconducting $Ta_3B_2@Ta_2O_5$ heterostructure with enhanced photocatalytic activity have been prepared by in-situ solid state reaction, using Ta_2O_5 and $NaBH_4$ powders. As-prepared $Ta_3B_2@Ta_2O_5$ products were characterized by XRD, FESEM, HRTEM, EDS, XPS and UV-vis absorption. The results showed that (210) crystal surface of Ta_3B_2 have tightly combined with (001) crystal surface of Ta_2O_5 to form a core-hell heterostructure. From the photocatalytic activity test, there is about 80 % of methylene blue (MB) being photodegraded in 180 min over $Ta_3B_2@Ta_2O_5$, which is about two times higher than that of pure Ta_2O_5 commercial powder ~ 38%. It is worthy pointing out that the enhanced photocatalytic activities originate from the metallic layer of interface and Ta_3B_2 nanodots. This special construction could accelerate electron mobility, increase visible light harvesting and enhance electron-hole separation ratio. Therefore, the $Ta_3B_2@Ta_2O_5$ heterostructure as a promising photocatalyst should have potential applications in removal of environmental pollution.

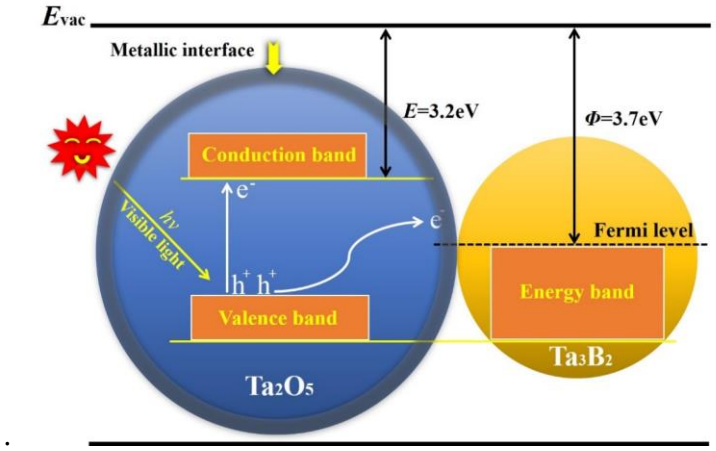

Fig.1 Proposed mechanism of the Ta_3B_2@Ta_2O_5 heterostructure enhanced photodegradation of MB under visible light irradiation.

References

[1]. K. L. Li, W. Cui, J. Y. Li, Y.J. Sun Y.H. Chu, G.M. Jiang, Y. Zhou, Y. X. Zhang, F. Dong, Tuning the reaction pathway of photocatalytic NO oxidation process to control the secondary pollution on monodisperse Au nanoparticles@g-C_3N_4, Chem. Eng. J. 378 (2019) 122184(1-9).

[2]. K. Vikrant, K.H. Kim, A. Deep, Photocatalytic mineralization of hydrogen sulfide as a dual-phase technique for hydrogen production and environmental remediation, Appl. Catal. B-Environ. 259 (2019) 118025(1-19).

$Sc_{0.28}Ti_{0.72}Fe_{2-x}T_x$ alloys with T = Mn or Co: phase diagrams and magnetocaloric effect

Sun-Liting, H. Yibole, O. Tegus and F. Guillou

Inner Mongolia Key Laboratory for Physics and Chemistry of Functional Materials, Inner Mongolia Normal University, Hohhot 010022, China

Email: 1076425849@qq.com

Abstract: Below their Curie temperature ($T_C \approx 325$ K), (Sc,Ti)Fe_2 Laves phases show a relatively unique case of first-order ferro-ferromagnetic transition ($T_{t1} \approx 70$ K) originating from an instability of the Fe moment [1,2]. We investigated the magnetocaloric effect and magnetoresistance of the ternary alloy $Sc_{0.28}Ti_{0.72}Fe_2$ and found that these two effects are larger at the ferro-ferromagnetic transition T_{t1} than at the Curie temperature [3].

We suggested a strategy to improve the magnetocaloric properties by bringing the transition at T_{t1} close to T_C and tested its possible realization by Co or Mn for Fe substitutions. This led us to explore for the first time the structural and magnetic phase diagrams of $Sc_{0.28}Ti_{0.72}Fe_{2-x}T_x$ quaternary alloys with T = Mn or Co. Substitutions on Fe by adjacent Mn or Co elements trigger opposite changes on the crystal structure, but both lead to a progressive disappearance of long-range ferromagnetic order and finite moment magnetism.

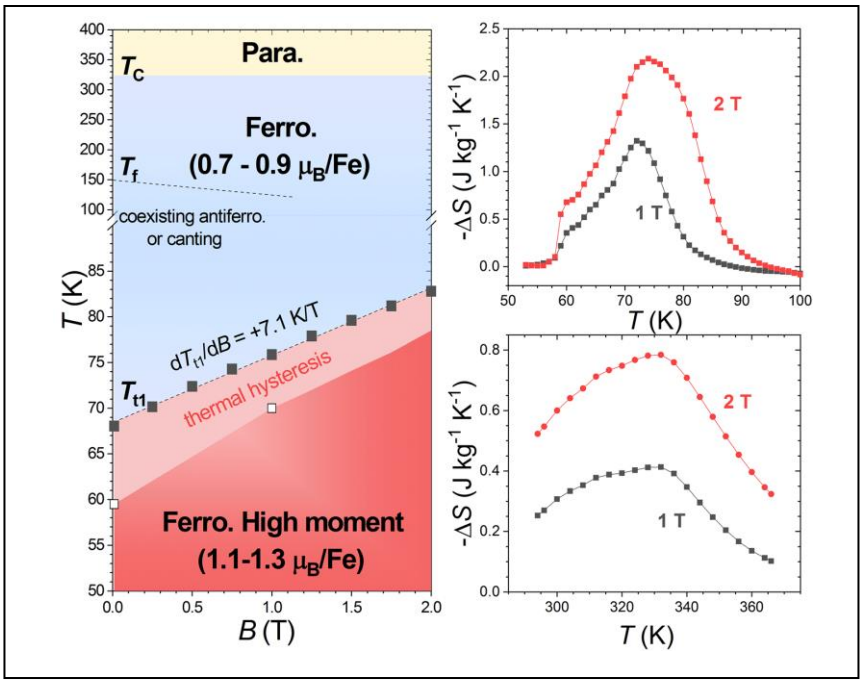

Fig.1. Magnetic phase diagram of $Sc_{0.28}Ti_{0.72}Fe_2$ (left) and magnetocaloric effect at the two magnetic transitions T_{t1} and T_C (right).

References

[1]. Y. Nishihara, Y. Yamaguchi, *J. Phys. Soc. Japn.* **54**, 1122 (1985).

[2]. M. Saoudi, J. Desportes, B. Ouladdiaf, *J. Mag. Mag. Mater.* **231**, 265 (2001).

[3]. Sun-Liting, H. Yibole, O. Tegus and F. Guillou, *Crystals* **10**, 410 (2020).

Origin of Anisotropy in Gadolinium Crystal

Dan Wei[1, 2], Zhibin Chen[1], Hui Yang[1], Yongjun Cao[1], and Chuan Liu[3]

[1]*College of Physics and Electronic Information, Inner Mongolia Normal University*

[2]*School of Materials Science and Engineering, Tsinghua University*

[3]*School of Physics, Peking University*

Email:20188038@imnu.edu.cn

Abstract: The first and second order anisotropy energies K_1 and K_2 of Gd crystal are calculated using a new spin Hamiltonian as in Eq.(1) and (2) [1,2,3] with the Hybrid Monte Carlo method [4,5].

$$\mathcal{H} = \frac{1}{2}\sum_i \boldsymbol{\Pi}_i^2 + \frac{\mathcal{F}[\{\boldsymbol{S}_i\}]}{k_B T} \tag{1}$$

$$\mathcal{F} = -\frac{1}{2}\sum_{\langle i,j\rangle} 2J\boldsymbol{S}_i\cdot\boldsymbol{S}_j + \frac{b}{4}\sum_i \left(\boldsymbol{S}_i^2 - S_0^2(T)\right)^2 + \frac{1}{2}\sum_{\langle i,j\rangle}^{\in(xy)} C_1\left(3(\boldsymbol{S}_i\cdot\hat{\boldsymbol{r}}_{ij})(\boldsymbol{S}_j\cdot\hat{\boldsymbol{r}}_{ij}) - \boldsymbol{S}_i\cdot\boldsymbol{S}_j\right)^2 + \frac{1}{2}\sum_{\langle i,j\rangle}^{\ni(xy)} C_2\left(3(\boldsymbol{S}_i\cdot\hat{\boldsymbol{r}}_{ij})(\boldsymbol{S}_j\cdot\hat{\boldsymbol{r}}_{ij}) - \boldsymbol{S}_i\cdot\boldsymbol{S}_j\right), \tag{2}$$

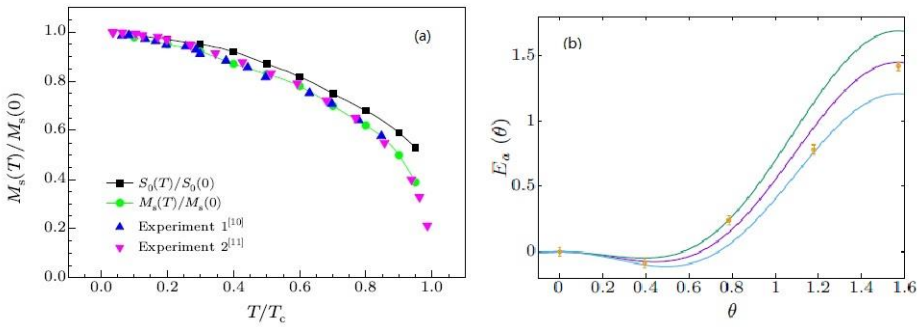

Fig. 1 (a) Calculated scaled saturation versus T compared with experiments, with J/k_BT_c~0.1; (2) the total energy density excluding the Zeeman energy versus the angle of the external field

The isotropic exchange J/k_BT_c and $S_0(T)$ are determined by fitting experiments of $M_s(T)$, as shown in Fig.1(a). It is found that, when the anisotropy of exchange interaction C_1 and C_2 are both zero, the total energy density

excluding the Zeeman energy is isotropic (err~10^{-2}erg/cm^3). The measured K_1 and K_2 of Gd [6] at low temperatures can be explained with $C_1/k_BT_c \sim 5\times10^{-7}$ and $C_2/k_BT_c \sim -10^{-5}$, with the corresponding energy density versus θ in Fig.1(b).

References

[1]. J. H. Van Vleck, *Phys. Rev.*, **52**, 1178 (1937).

[2]. L. Nèel, *J. Phys. Radium.*, **15(5)**, 376 (1954).

[3]. D. Wei, Z. Chen, H. Yang, Y. Cao, C. Liu, *Chin. Phys. Lett.*, **37(5)**, 057501 (2020).

[4]. S. Duane, A. D. Kennedy, B. J. Pendleton, D. Roweth, *Phys. Rev. B*, **195**, 216 (1987).

[5]. D. Wei, J. Song, C. Liu, *IEEE Trans. Magn*, **52(11)**, 7100808 (2016).

[6]. C. D. Graham Jr., *J. Appl. Phys.*, **34(4)**, 1341 (1963).

Magnetic properties of flux grown $MnFe_4Si_3$ single crystal

H. Yibole[1], W. Hanggai[1], Z.Q. Ou[1], O. Tegus[1], F. Guillou[1]

[1]Inner Mongolia Key Laboratory for Physics and Chemistry of Functional Materials, *Inner Mongolia Normal University, 81 Zhaowuda Rd, Saihan District, Hohhot 010022, China*

Email: hyibole@imnu.edu.com

Abstract: Transition metal based compounds $Mn_{5-x}Fe_xSi_3$ are currently receiving a renewed interest for their rich magnetic properties and for their potential use in magnetocaloric applications [1-2]. Despite numerous investigations, some controversies persist on $MnFe_4Si_3$ and related materials, in particular on the Ehrenfest classification of the magnetic transition and the magnetocrystalline anisotropy configuration. Here, magnetic, magnetocaloric properties and the magnetic anisotropy of $MnFe_4Si_3$ are investigated on a high quality single crystal grown by flux method, and the results compared to polycrystalline materials. In contrast to former literature, our detailed analysis of the magnetocaloric effect demonstrates that the ferromagnetic transition is of second-order, in line with the absence of thermal hysteresis at the transition [3]. We also conduct one of the first quantitative estimate of the magnetic anisotropy parameters in the $Mn_{5-x}Fe_xSi_3$ material family.

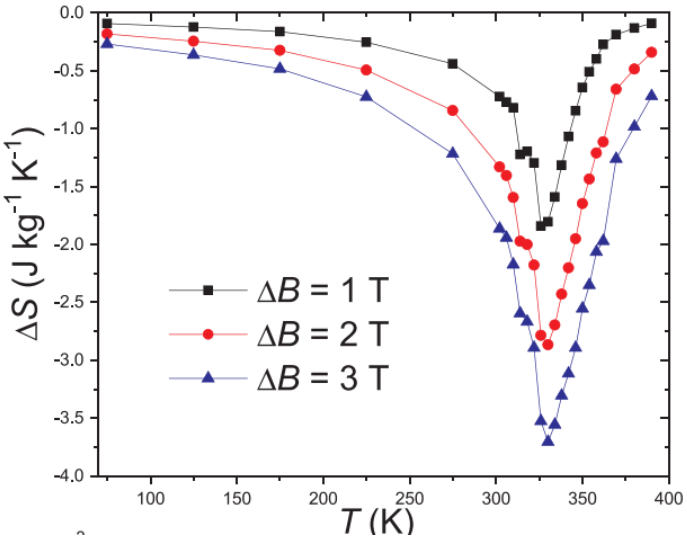

Fig. 1. Magnetocaloric effect (isothermal entropy change) of $MnFe_4Si_3$ single crystal measured along the easy magnetization direction.

References

[1]. Dagula, Songlin, O. Tegus, E. Brück, J.C.P. Klaasse, F.R. de Boer, K.H.J. Buschow, *J. Alloys Compds.* **334**, 249–252(2002).

[2]. P. Hering, K. Friese, J. Voigt, J. Person, N. Aliouane, A. Grzechnik, A. Senshyn,T. Brückel, *Chem. Mater.* **27**, 7128 (2015).

[3]. H. Yibole, W. Hanggai, Z.Q. Ou, R. Hamane, V. Hardy, F. Guillou, *J. Mag. Mag. Mater.* **504** 166597 (2020)

Elastic theory for self-formed 3D nano-/micro- architectures

B. Narsu

Inner Mongolia Key lab of Physics and Chemistry of Functional materials, & College of Physics and electronic information, Inner Mongolia normal University, Hohhot 010022, China

Abstract: The self-formed 3D nano-/micro-architectures have great potential applications in high performance electronics, photonics, mechanics, sensors , energy storage, thermoelectric and micro-/nano-electromechanical systems (MEMS/NEMS) [1-2]. Fabrication of nano-/micro-architectures manipulates ultrathin nanstructures by strains relaxation, thermal stress as well as surface stress [3-5]. Therefore, a rigorous and universal nanomechanical theory of nanostructures is a critical tool for the precision design and engineering of nano-/micro-architectures. An elastic theory for bending, curling, buckling and vibration of nanofilm and nanowires is established according to the experimental observation that the elastic modulus and surface energy as well as surface stress of nanostructures are size dependent [6]. Our theory can reproduce available experimental results nicely, and hence we believe that this theory can be serve as a predictive tool for nano-/ micro architectures.

Financial support of National natural science Foundation under grant 11864030, 50906039 & 11464037 is acknowledged.

References

[1] Dahl-Young Khang, Hanqing Jiang, Young Huang, John A. Rogers. A Stretchable Form of Single-Crystal Silicon for High-Performance Electronics on Rubber Substrates. Science, 311, 208-212 (2006).

[2] Zi Chen, Gaoshan Huang, Ian Trase, Xiaomin Han, and Yongfeng Mei. Mechanical Self-Assembly of a Strain-Engineered Flexible Layer: Wrinkling, Rolling, and Twisting. Phys. Rev. Appl. 5, 017001 (2016)

[3] S. Mendach, R. Songmuang, S. Kiravittaya, A. Rastelli, M. Benjoucef, and O. G. Schmidt, Appl. Phys. Lett. 88, 111120 (2006).

[4] J. Zang, M. H. Huang and F. Liu. Mechanism for Nanotube Formation from Self-Bending Nanofilms Driven by Atomic-Scale Surface-Stress Imbalance. Phys. Rev. Lett. 98 146102 (2007);

[5] Wen Huang, Seid Koric, Xin Yu, K. Jimmy Hsia, and Xiuling Li. Precision Structural Engineering of Self-Rolled-up 3D Nanomembranes Guided by Transient Quasi-Static FEM Modeling. Nano Lett. 2014, 14, 11, 6293–6297.

[6] Q. Jiang and H.M. Lu. Size dependent interface energy and its applications Surface Science Reports 63, 427–464 (2008)

[7] Miao Liu and Feng Liu. Quantum manifestation of elastic constants in nanofifilms. Nanotechnology, 25, 135706 (2014)

[8] Jiangang Li, B Narsu, Guohong Yun and Haiyan Yao. Elasticity theory of ultrathin nanofilms. J. Phys. D: Appl. Phys. 48 285301 (2015) .

Study on phase stabilization of black phosphorene

T. Bao[1,2]*, X. Tian[1,2], Narengerile[1,2] and O. Tegus[1,2]

[1] *College of Physics and Electronic Information, Inner Mongolia Normal University, Hohhot, 010022, China*

[2]*Inner Mongolia Key Laboratory for Physics and Chemistry of Functional Materials, Inner Mongolia Normal University, Hohhot, 010022, China*

E-mail: tanaph@imnu.edu.cn

Abstract: The black phosphorus crystals and black phosphorene are prepared from amorphous red phosphorus by mechanical ball milling-liquid stripping method. The spectrophotometric analysis shows that a few layers of black phosphorene have been successfully prepared. Aiming at the characteristics of black phosphorene that was easily degraded in the natural environment, a low-cost solvothermal method was used, and black phosphorene and nickel chloride are used as raw materials to prepare a green and pollution-free transition metal phosphide heterojunction was prepared. Metal ions are preferentially deposited on the edges and defects of black phosphorene and unsaturated sites, forming a black phosphorene / transition metal phosphide (BP / Ni_2P) in-plane heterojunction. It can repair defects and prevent the oxidation of black phosphorus.

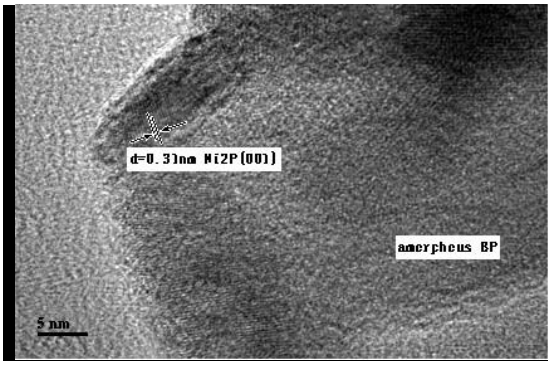

Fig. 1 Ni^{2+} ion forms a relatively stable Ni_2P at the edge after deposition on the two-dimensional black phosphorus surface

Study of order-disorder phase transitions in Cu-Au alloys using X-ray diffuse scattering

L.Enkhtor[1], V.M.Silonov[2], Ts.Gantulga[1], Kh.Balt-Erdene[3], A.Badmaarag[4]

[1]*National University of Mongolia, School of Science and Arts, Ulaanbaatar, Mongolia*

[2] *Moscow State University, Faculty of Physics, Moscow, Russia*

[3] *Mongolian University of Science and Technology, Physics Department, Ulaanbaatar, Mongolia*

[4]*Frank Laboratory of Neutron Physics, Joint Institute for Nuclear Research, Dubna, Russia*

Abstract: Short-range order parameters on the first three shells of Cu-10, 17 and 25 at. % Au alloys have been identified from X-ray diffuse scattering intensity by accounting microscopic static displacements of atoms on a particular shell. Pairwise interatomic potentials on the considered shells and critical temperature of disorder-order phase transition were calculated using values of short-range order parameters. An obtained value of critical temperature of disorder-order phase transition allows clarifying the phase diagram of the Cu-Au system.

Keywords: X-rays diffuse scattering; short-range order; static displacement of atoms; interatomic quasi elastic forces; pairwise interatomic potential; critical temperature of disorder-order phase transition

$Li_4Ti_5O_{12}$/graphene composite as anode for li-ion batteries

L.Sarantuya*[1], N.Tsogbadrakh**[2], A.Munkhbaatar[1], G.Sevjidsuren[1], P.Altantsog[1]

[1] *Institute of Physics and Technology, Mongolian Academy of Sciences, Ulaanbaatar 13330, Mongolia,*

[2]*Department of Physics, National University of Mongolia, Ulaanbaatar 14201, Mongolia,*

*e-mail: * saraa.ipt@gmail.com, **tsogbadrakh@num.edu.mn*

Abstract: We investigated the effects of graphene doping on the structural and electronic properties of an anode material spinel $Li_4Ti_5O_{12}$ for lithium ion batteries. Spinel structured $Li_4Ti_5O_{12}$ has poor intrinsic electronic properties. In order to enhance it, a graphene was used, as additional composition. The $Li_4Ti_5O_{12}$/graphene composites have been successfully synthesized by reduction process of graphene oxide via hydrothermal treatment. The morphology, crystal structure and elemental compositions of the prepared composites are characterized by Scanning Electron Microscopy (SEM), Transmission Electron Microscopy (TEM), X-Ray diffraction (XRD), Fourier transform Infrared spectroscopy (FT-IR) and Thermogravimetric Analysis (TGA). The $Li_4Ti_5O_{12}$/graphene composites exhibit a well-defined cubic spinel structure with an average particle size of approximately 400-500 nm. In the present study, in order to understand the effects of graphene coatings adsorbed on the surface of $Li_4Ti_5O_{12}$, we have predicted by the first principles calculations based on the density functional theory (DFT).

Keywords: Li-ion battery $Li_4Ti_5O_{12}$/graphene composites, DFT, first principles calculations.

Density functional calculation of excited states of atoms using CWDVR approach

D. Naranchimeg[1], G. Munkhsaikhan[1], L.Khenmedekh[1], N.Tsogbadrakh[2], O.Sukh[1]

[1]*Department of Physics, School of Applied Sciences, Mongolian University of Science and Technology, Ulaanbaatar 14191, Mongolia.*

[2]*Department of Physics, School of Arts and Sciences, National University of Mongolia, Ulaanbaatar 14201, Mongolia*

E-mail: naranchimeg@must.edu.mn

Abstract: A density-functional approach for the calculation of singly, double excited states of atomic system have been calculated using a nonvariational, exchange potential within the nonrelativistic Hohenberg-Kohn-Sham density functional theory (DFT). The self-consistent Kohn-Sham equations for many-electron atoms are solved using the Coulomb wave function Discrete Variable Method (CWDVR). The gradient-free representation functional is used to incorporate exchange functional.

The discrete variable method is used for the uniform and optimal spatial grid discretization and solution of the Kohn-Sham equation. The equation is numerically solved using the CWDVR method. First time we have reported the solution of the Kohn-Sham equation on the excited state problem for the He, Li, Be atoms by the CWDVR method. Our results suggest that CWDVR approach shown to be an efficient and precise solution of excited state energies of atoms.

We illustrate that the calculated electronic energies for corresponding atoms are in good agreement with other best available values. Estimating the energies and splitting of the 1s2s singlet and triplet states of atoms yields qualitatively correct results. Using a sixline computer program, the 1s2s energies calculated by matrix diagonalization using a seven-state basis improve the results to 0.4% error or better.

A single-Slater-determinant energy of the electronic configuration is calculated by using these electron spin orbitals. Finally, a multiplet energy of an excited state is evaluated from the single-Slater-determinant energies of the electronic configurations involved in terms of Slater's diagonal sum rule.

Keywords: Density Functional Theory, Effective potential, Electronic structure.

Design of experiments in optimization of motor parameters

Ariunbolor Purvee

German-Mongolian Institute for Resources and Technology (GMIT), Mongolia

Abstract: The most popular type of motors in use are squirrel-cage induction motors. Electrical, mechanical, and electromagnetic behaviors of actual induction motors need to be understood in order to understand key frequencies of motors with and without faults. Experiments on motors, conducted in a laboratory setting, are expensive and limited because the motor should be broken to create the fault to be studied. Another motor is again needed to be broken to study a different fault. Large capacity motors are generally not allowed to break because of cost and safety factors. Therefore, it is better to study the actual motor on a computer. It is called simulated motor if the actual motor is studied on a computer. A simulated motor saves an enormous amount of time and money. Motors of any capacity, with any type of fault, can be studied if a motor could be simulated in Simulink MATLAB or other software. But, the output values of the simulated motor are very close to the values on the nameplate of the actual motor for being exactly the same motors. Therefore, the goal of this paper is to find the optimum input parameters that make the minimum difference between outputs and targets by using an excel spreadsheet as evaluated by the Taguchi method and Grey relational analysis. The Taguchi method and Grey relational analysis are defined separately in the study. The new equation was developed based on this study. The output values were obtained without using software programming based on the new equation developed during the research work. Therefore, the Taguchi method and Grey relational analysis are able to be calculated using Excel. The results of the paper are that the outputs of the simulated motor were almost identical to the nameplate data on actual motor, indicating that our methods and models can be used to simulate a healthy motor, allowing us to now use our simulation to examine motor faults experimentally.

Keywords: Grey relational analysis, Taguchi method, faults, rotor bar, model, simulation, Excel.

Preparation of porous material from Mongolian clay minerals

Gendenjamts Oyun-Erdene[1, A], Dolgormaa Anudari[1],
Luvsandagva Mandakhsaikhan[1], Zoodol Zolzaya[1], Jadambaa Temuujin[1, B]
[1]*Institute of Chemistry and Chemical Technology, Mongolian Academy of Sciences*
Peace Ave., 51, Ulaanbaatar 13330, Mongolia
[a]*oyunerdeneg@mas.ac.mn,* [b] *temuujin@mas.ac.mn*

Abstract: Porous materials have been prepared from various clay minerals by selective acid leaching. Acid activation is the most commonly used method to enhance the chemical and physical properties of clay minerals. Acid leaching has been using to increase the surface area of clay minerals and to obtain solids with high porosity and a large number of acidic sites. This paper is focused mostly on the results of acid leaching of Mongolian clay minerals (montmorillonite and muscovite) in our laboratory. The influence of acid concentration and leaching time on the porous properties of silica was studied. After pre-treatment of the montmorillonite by simple physical purification methods, it was autoclaved with a 10% hydrochloric acid solution at 120°C for 10h. Muscovite was milled with a vibratory mill for 5 minutes to destroy sheet structure. Then the milled sample was passed a sieve with 1 mm and used for the leaching experiments. Leaching was performed hydrochloric acid with 2.5M concentration at 90°C for up to 20min.

X-ray diffraction (XRD), X-ray fluorescence analysis (XRF), Fourier transform infrared spectroscopy (FTIR), scanning electron microscopy (SEM), and specific surface area (SSA) used for the raw and leached samples. The specific surface area is the main characteristic of porous materials, and the surface area of leached montmorillonite increased up to 77% and muscovite up to 18%.

Keywords: montmorillonite, muscovite, acid leaching, porous materials

Synthesis of Silver Nanoparticles by Hydrothermal Processing

E. Surenjav[1*], B. Buyankhishig[1], N. Byamba-Ochir[1], N. Davaadorj[1], S. Zhiqiang[2] and O. Tegus[2]

[1]*Institute of Chemistry and Chemical Technology, Mongolian Academy of Sciences, Ulaanbaatar 13330, Mongolia*

[2]*Inner Mongolia Key Laboratory for Physics and Chemistry of Functional Materials, Hohhot 010022China*

**e-mail: enkhtuul@mas.ac.mn*

Abstract: Hydrothermal water treatments of silver acetate (CH_3COOAg) were investigated to reveal the factors controlling the formation of silver nanoparticles (AgNPs) with uniform size distribution. The effect of reaction time and concentration of silver acetate solution on the synthesis of Ag nanoparticles were studied, and fabricated products are characterized. The hydrothermal water treatments of CH_3COOAg were carried out between the temperatures of 250 - 450^oC in a batch reactor. In supercritical water regions, at 400^oC temperature and 31MPa pressure, silver particles are rapidly synthesized due to reaction rate increases at a low dielectric constant of supercritical water. The preparation of the silver particles with 30-80 nm in size showed a highly crystalline structure identified by XRD and TEM observations.

Keywords: silver nanoparticles, supercritical water treatment, particle size

Metallic thickness optimization of a monometallic plasmonic structure for a surface-plasmon resonance biosensor

E.Nomin-Erdene[1], Ts.Khos-Ochir[1], A.Nomin[2], B.Khishigsuren[2], B.Zaya[2], O.Oidovsambuu[2], J.Davaasambuu[1]

[1]*Laser Research Center, National University of Mongolia*

[2]*Laboratory of Genetic Engineering, National University of Mongolia*

Abstract: Surface-plasmon resonance (SPR) effect in thin metal films is highly sensitive to the dielectric refractive index changes in the vicinity of metal interface and the conventional Kretschmann configuration has been widely used in the SPR measurement. In this work we have presented the metallic thickness optimization for a monometallic plasmonic structure using the prism-based Kretschmann configuration in angular and spectral interrogation. He-Ne laser with wavelength of 632.8 nm as an optical source, a thin gold layer deposited onto the glass substrate and a BK7 glass prism were applied for this studies.

Based on the numerical analysis with variation of metallic layer thickness, angle of incidence and wavelength we will obtain the resonance parameters, such as reflectivity and phase. Experimentally, the SPR spectra of a pure gold sensing surface has been studied. With functionalizing with specific antigen molecules on the surface of the gold layer, this optimized settings can be further used as biosensing purpose for detection of certain analytes.

This work was supported by NUM Fellowship Research Project Code Number: P2019-3738.

Thermal coatings for tribologically highly loaded parts of pump

Ariunbolor Purvee[1], Gunther C. STEHR[2], Battsengel Baatar[1]

[1] *German-Mongolian Institute for Resources and Technology (GMIT), Mongolia*

[2]*HTW Dresden University of Applied Sciences Faculty of Mechanical Engineering, Germany*

Abstract: This paper presents the results of a research study of two parts of pumps with different laser thermal coatings that are used to restore the dimensions of components that have been worn or corroded of tribological highly loaded machines or rotation equipment. Based on the application of Metal Matrix Composite (MMC) materials investigated by South Dakota School of Mines and Technology, USA, three selected coatings with a very high amount of the hard phases (carbides) on impeller blades were applied.

After coating, these pump parts were used under real production conditions in a mineral processing plant in Mongolia. This research study investigated the wear resistance of the coated impeller blades in comparison to the uncoated version within the same impeller, in a practical trial of 456 h of operation time. While the uncoated impeller blade suffers a material loss of between 16 and 28 mm, the coatings were rubbed off by approx. 0.8 to 1.5 mm. Even if the coatings are afflicted with clearly visible cracks, the metallurgical bond to the substrate material, and thus the layer adhesion, is flawless. While white cast iron as a substrate material is considered as non-weldable due to the chemical composition, the application of laser thermal coatings opens the way to coat these original materials. The coatings were merely straightened out by the wear, and survived many more hours of practical use. We roughly estimated the material removal of the coated impeller blades to the uncoated impeller blade to be about 1:10. A cover plate experiment did not proceed successfully due to base material failure. For an explanation of the success of the coatings, the hardness ratio of the copper ore particles versus the hardness of the part, materials (coatings) plays an important role. With the very hard

carbides embedded in the hard matrix material of the coatings, we could move the abrasive wear behavior from the high-level status to the low-level status.

Keywords: laser, substrate material, impeller blades, chemical composition, welding

Improvement of imaging and image correction methods of soft X-ray projection microscopy

Duurenbuyan Baatar[1, 2, *], Erdenetogtokh Jamsranjav[1], Vanchinkhuu Jigmeddorj[2], Tatsuo Shiina[3], Yasuhito Kinjo[4], Atsushi Ito[4]

[1]*Institute of Physics and Technology, Mongolian Academy of Sciences, Ulaanbaatar, Mongolia*

[2]*School of Art and Sciences, National University of Mongolia, Ulaanbaatar, Mongolia*

[3]*Graduate School of Advanced Integration Science, Chiba University, Chiba-shi, Chiba, Japan*

[4]*School of Engineering, Tokai University, Hiratsuka-shi, Kanagawa, Japan*

**E-mail: duurenbuyanb@mas.ac.mn*

Abstract: Soft X-ray microscopy has been developed for high resolution imaging of hydrated biological specimens due to the availability of water window region. In particular, a projection type microscope has a number of advantages in wide viewing area, easy zooming function and easy extensibility to CT (Computed Tomography). The blur of projection image due to the diffraction of X-rays, which eventually reduces spatial resolution, could be corrected by an iteration procedure, i.e., repetition of Fourier and inverse Fourier transformations. However, it was found that the correction is not sufficiently effective for all images, especially for chromosome images with low contrasts. In the recent study, we could capture relatively high contrast images of chromosomes staining them by Platinum blue (Pt-blue). We also increased contrast of the projection images by using noise removal and contrast enhancement methods. As a result, the chromosome images with low magnifications were corrected effectively.

Keywords: Soft X-ray, Pt-blue, Iteration procedure, Chromosome, Latex particle

$Gd_3Al_4GaO_{12}:Cr^{3+}$ Phosphors for Far-Red Light Emitting Diodes

Xiang Li[1], Dahai Hu[1],Yizhi Ma[1],Xinran Wan[1],Fengxiang Wan[1], Zhiqiang Song[1], Qier Sa[1]and Kefu Chao[1]

[1]*Inner Mongolia Key Laboratory of Physics and Chemistry of Functional Materials, College of Physics and Electronic Information, Inner Mongolia Normal University*

E-mail: phyerick@imnu.edu.cn

Abstract: Recently, Far-Red Light Emitting Diodes have attracted considerable interest in the research field worldwide. Emerging phototherapy in a clinic as well as plant photomorphogenesis call for efficient red/far-red light resources to target and/or actuate the interaction of light and living organisms. Here, Fabrication of Cr^{3+}doped $Gd_3Al_4GaO_{12}$ phosphors significantly promotes the potential applications by efficiently converting blue excitation light of a commercial InGaN chip to far-red broadband emission in the 640-850 nm region,which is the result of the transition of Cr^{3+} $^4T_2 \rightarrow {}^4A_2$ level. A sharp emission peak at 693nm is the R line belonging to Cr^{3+} in $Gd_3Al_4GaO_{12}$ garnet. As the Cr^{3+} doping concentration increases, the luminous intensity of the sample increases first and then decreases. When the doping concentration of Cr^{3+} is 0.1mol phosphor,the luminous intensity is strongest at 712nm .Based on luminescence and temperature-dependent stability and decay, energy transfer models are rationally established, The current exploration will pave a promising way to engineer $Gd_3Al_4GaO_{12}:Cr^{3+}$ activated optoelectronic devices for all kinds of photobiological applications.

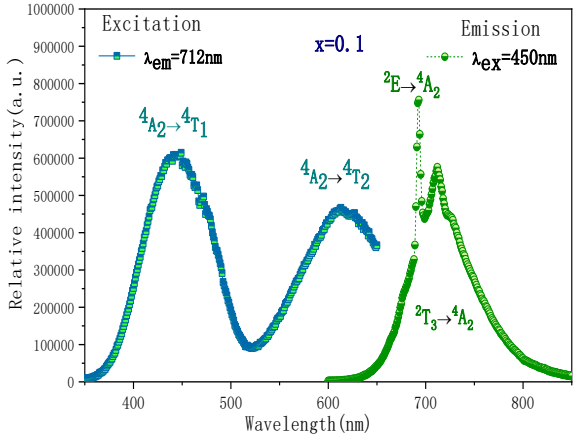

Fig.1. Excitation and emission spectra of $Gd_3Al_4GaO_{12}$：Cr^{3+} phosphors

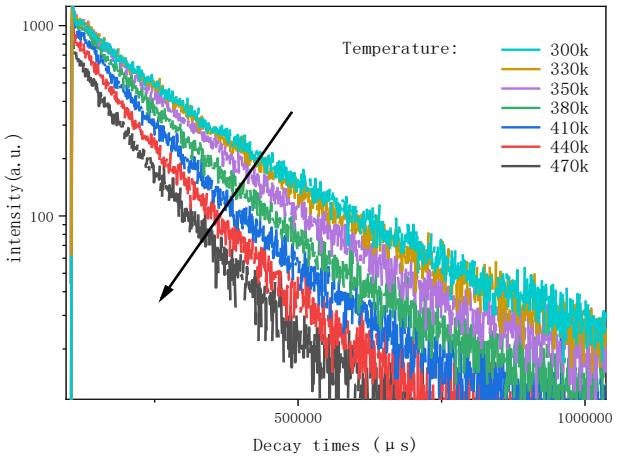

Fig.2.Decay curves of $^4T_2 \rightarrow {}^4A_2$ of $Gd_3Al_4GaO_{12}$：Cr^{3+}phosphors against temperature

References

[1]. [S. Liu, P .Sun, Y. Liu, T .Zhou, S. Li, R. Xie, X. Xu,R. Dong, J .Jiang, H. Jiang, *ACS Appl. Mater. Interfaces*, **11**, 2130-2139(2019)

[2]. V. Rajendran, M. Fang,G .Guzman, T. Lesniewski, S. Mahlik, M. Grinberg, G. Leniec, S. Kaczmarek, *ACS Energy Lett* ,**3**, 2679-2684(2018)

Bonding effects on the crystal structure, magnetic and mechanical properties of Fe_2P-based Mn-Fe-P-Si compound

Jiaying Zhang[1], Dan Zhao[1], and Zhiqiang Ou[1, 2]

[1] *School of Physics and Electronic Information, Inner Mongolia Normal University, Inner Mongolia, Hohhot 010020, China;*

[2] *Inner Mongolia Key Laboratory for Physics and Chemistry of Functional Material, Inner Mongolia Normal University, Hohhot 010022, China*

Email: ouzhiqiang_nsd@hotmail.com

Abstract: In this paper, the $Mn_{1.25}Fe_{0.65}P_{0.50}Si_{0.50}$ compound was prepared by mechanical alloying. The planetary ball mill, X-ray diffractometer, scanning electron microscope, thermal gravimetric analyzer and vibrating sample magnetometer and were employed. The structure of the sample and the magnetism of the sample were measured and analyzed. The experimental results show that epoxy resin bonding has no influence on the crystal structure, Curie temperature and thermal hysteresis, the values for Curie temperature and thermal hysteresis are 271 and 4.5 K, respectively. The compressive strength of Al-doped samples increased by about 68 % from P = 161 MPa for epoxy-free bulk sample to P = 270 MPa for the sample with 5 wt.% epoxy one.

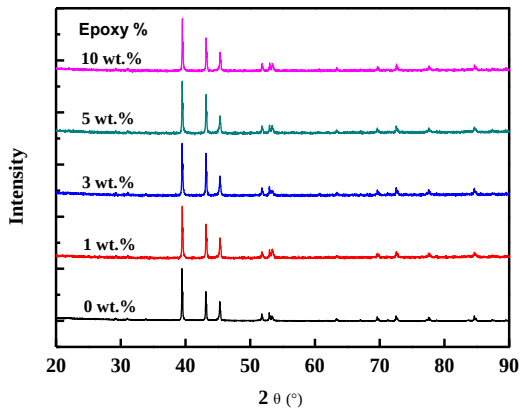

Fig. 1 X-ray diffraction pattern of for the bonded $Mn_{1.25}Fe_{0.65}P_{0.50}Si_{0.50}$ with different epoxy resin content.

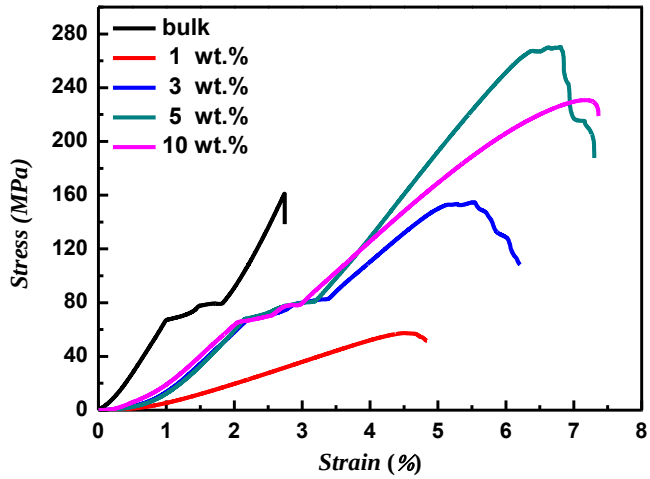

Fig. 2 Compressive stress-strain curves for the bonded $Mn_{1.25}Fe_{0.65}P_{0.50}Si_{0.50}$ with different epoxy resin content in comparison with bulk compound.

References

[1]. O. Tegus, E. Brück, K.H.J Buschow, F.R. de Boer, *Nature*, **415,** 150 (2002).

[2]. H. Zhang, etc, *Applied Physics Letters*, **104**, 062407 (2014).

Dynamic potential deposition of CuGa oxides

Linrui Zhang[1], Bingqing Zhou[1]

[1]*College of Physics and Electron Information, Inner Mongolia Normal University, Hohhot 010022, China*

Email:415131777@qq.com

Abstract: In the preparation of CIG precursor, Ga oxide deposition is one of the effective methods to solve the difficulty of Ga deposition. In this experiment, the CuGa oxide was deposited by dynamic potential deposition. The influence factors of electro-depostion such as potential intervals，deposition time were studied. The results show that CuGa oxides co-deposition will intensify the hydrogen evolution reaction compared with the Ga single element deposition. In addition, the homogeneity of precursors prepared by dynamic potential deposition is better than that of CuGa oxide prepared by potentiostatic deposition. Cu-Ga oxide growth varied with different potential intervals, which shows plane, dendritic and particle topographies. Meanwhile, with the increase of deposition time, the content of precursor elements increased linearly, and the reaction under dynamic potential showed a certain stability.

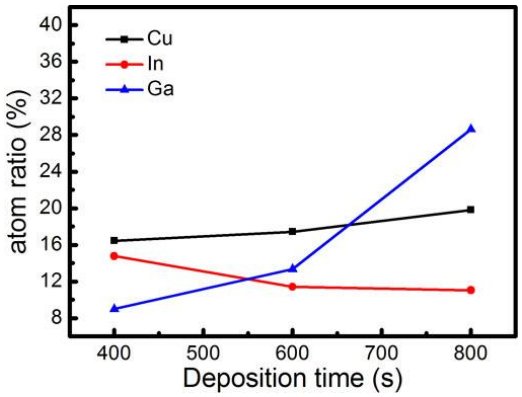

Fig. 1. Atomic number ratio of elements in precursors prepared at different deposition time of CuGa oxide

References

[1]. A. Duchatelet, G. Savidand, R. N. Vannier, E. Chassaing, D. Lincot, J. Renew. Sustain. Ener(American), 5, 011203 (2013).

[2]. A. Duchatelet,z G. Savidand,a N. Loones, E. Chassaing, D. Lincot, J. Electrochem. Soc(American), 161, D3120-D3129 (2014).

[3]. A. Duchatelet, T. Sidali, N. Loones, G. Savidand, E. Chassaing, D. Lincot, Sol. Energy Mater. Sol. Cells(American),119, 241-245 (2013).

XRD and EXAFS Study on Preparation Process of the $Mn_{125}Fe_{70}P_{50}Si_{50}$ Compound

Yingjie Li [1], YuanjieHao[2], Zhiqiang Ou[1], O Tegus[1], Ikuo Nakai[3]

[1] *Inner Mongolia Key Laboratory for Physics and Chemistry of Functional Materials, Physics and Electronic Information College, Inner Mongolia Normal University, Hohhot 010022, China*

[2]*Key Laboratory of Materials Modification by Laser, Ion and Electron Beams, Chinese Ministry of Education, School of Physics, Dalian University of Technology, Dalian 116024, China.*

[3]*Department of Electrical and Electronic Engineering, Tottori University, Tottori 680-8552, Japan*

Email:lyingjie@imnu.edu.cn

Abstract: In recent years magnetic refrigeration has attracted much attention as an energy saving and environmentally friendly alternative to conventional vapor-compression refrigeration.[1, 2] More recently, Fe_2P type $Fe_{2-x}Mn_x(P,Si)$ compounds have been intensively investigated as a promising candidate material for room temperature magnetic refrigeration. [3] In present work, from XRD and XAFS measurements, we investigate the ball milling preparation process of the $Mn_{125}Fe_{70}P_{50}Si_{50}$ compound. The proper amounts of Mn (99.9%), Fe (99.5%), Si (99.99%), and red-P (99.999%) with the ratio of 125:70:50:50 were mixed and milled up to 220 h under vacuum (about 10^{-5}Pa). During milling we picked a piece of powders at 30 h, 60 h, 100 h, 170 h and 220 h. The XRD was measured using Cu K_α radiation in a conventional θ-2θ scan mode. The EXAFS measurements near Fe and Mn *K* edges were carried out using synchrotron radiation at the beamline BL9C of Photon Factory.[4] The storage ring was operated in the top-up mode at 2.5 GeV with a beam current of about 450 mA. The Si (111) double crystal monochromator was installed in the optics system. Figure1 represents the XRD patterns of milling

$Mn_{125}Fe_{70}P_{50}Si_{50}$ at 295 K. The typical indices of the reflections are labeled. For $Mn_{125}Fe_{70}P_{50}Si_{50}$ up to 100 h, the reflections of Mn (114) and Fe (011) are quite clear, although they gradually increase in width with milling. At 170 h, however, only a broad bump near about 44 degree is detected, and it becomes further indistinct at 220 h.

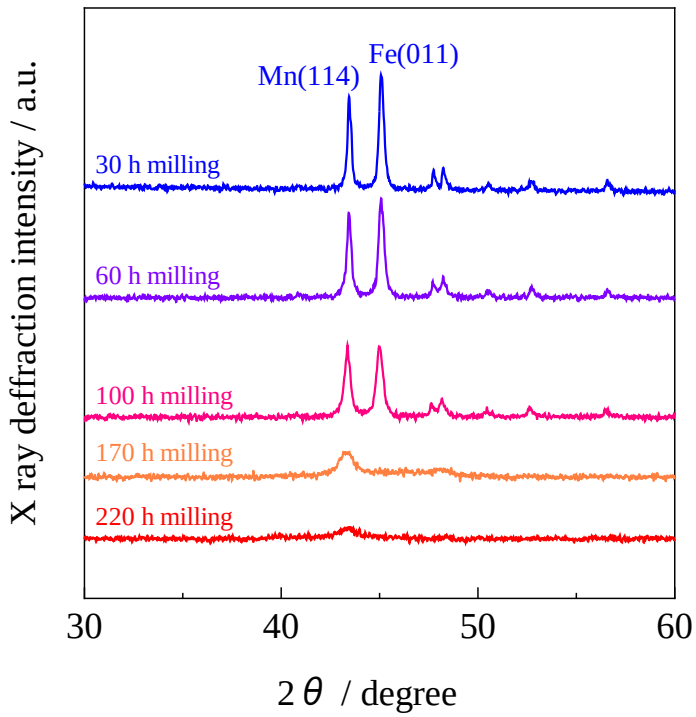

Fig. 1. XRD patterns of milling $Mn_{125}Fe_{70}P_{50}Si_{50}$ at 295 K.

The radial structure function derived from Fourier transformation of observed EXAFS oscillation $k^3\chi(k)$ is displayed in Figures 2 for milling $Mn_{125}Fe_{70}P_{50}Si_{50}$ at 295 K compared with the Mn metal. The radial structure function of 30 h, 60 h and 100 h milling samples are similar to that of the Mn foil. The spectra after 170 h milling are different from the Mn foil.

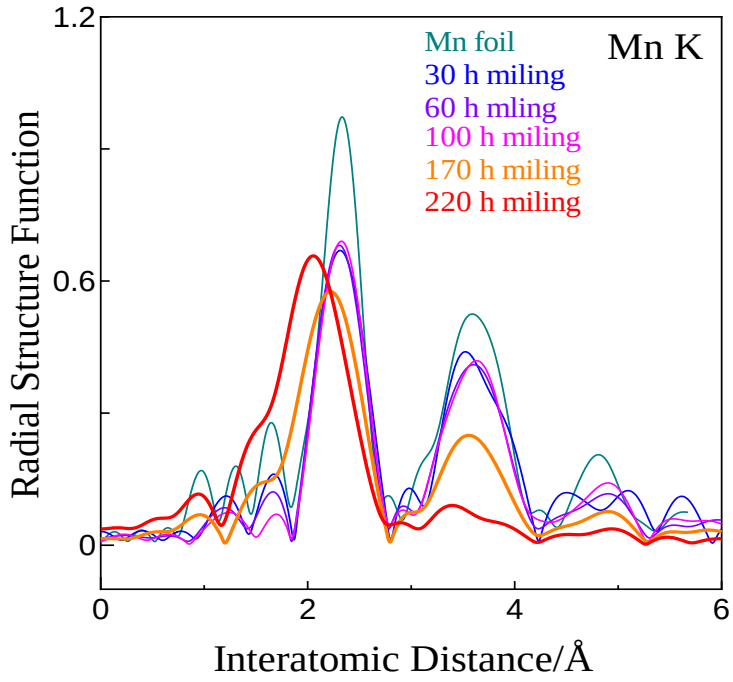

Fig. 2. The radial structure function of milling $Mn_{125}Fe_{70}P_{50}Si_{50}$ with Mn metal samples for the Mn *K* edge at 295 K.

We fit the Fourier filtering $k^3\chi(k)$ spectrum to the following formula using the least squares method,[5,6]

$$\chi(k) = \sum_i N_i \cdot |f_i(k,\pi)| \cdot \exp(-2(\sigma_i^2 k^2 + R_i/\lambda))/kR_i^2 \cdot \sin(2kR_i + \delta_i(k)), \quad (1)$$

Here N_i is the coordination number, $f_i(k, \pi)$ is backscattering amplitude, σ_i is the Debye-Waller factor, R_i is the interatomic distance between the absorbing and the *i*-th neighboring atom, δ_i is the phase shift and λ is the mean free path of photoelectron. At the meeting, we report the structural parameters of $Mn_{125}Fe_{70}P_{50}Si_{50}$ with different milling times.

This work was supported by China Science Foundation (No. 51161035). The XAFS measurement was performed under the approval of Photon Factory Program Advisory Committee (No. 2012G095, No. 2014G047, No. 2016G135, No. 2018G010).

References

[1]. E. Brück, *J. Phys. D: Appl. Phys*, **38** R381-391 (2005).

[2]. O. Tegus, E. Brück, K. H. J. Buschow, F. R. de Boer, *Nature*, **415** 150-152 (2002).

[3]. Y. X. Geng, O. Tegus, Q. Bilige, *Chin. Phys. B*,**21**037504:1-5 (2012).

[4]. M. Nomura, A. Koyama, *KEK Report***1** 95-15(1996).

[5]. D. E Sayers, E. A Stem and F. W Lytle, *Phys. Rev. Lett*, **27** 1204(1971)

[6]. F. Grandjean, G. J Long, R. Cortes, D. T Morelli and G. P Meisner, *Phys. Rev. B*, **62** 12569(2000)

Solubility and aggregation behavior of alanine magnesium complexes

Naren Gerile[1,2 *], Shi Yifeng[1], Zhang Ying[1], Tana Bao[1,2], O Tegus[1,2]

[1]*College of Physics and Electronic Information, Inner Mongolia Normal University, Huhhot 010022, China*;

[2]*Inner Mongolia Key Laboratory for Physics and Chemistry of Functional Materials, Inner Mongolia Normal University , Huhhot 010022, China*)

email: naren88@hotmail.com

Abstract: Two octyl amino acid magnesium metal complexes were synthesized and investigated in this study: magnesium(II) octanoyl-alaninate ($Mg(oct\text{-}L\text{-}ala)_2$), magnesium (II) octanoyl-phenylalaninate ($Mg(oct\text{-}L\text{-}phe)_2$). The molecular structure and surface morphology of these two complexes were studied using various methods, including ^1H NMR, FT-IR, powder XRD, and Scanning Electron Microscope (SEM). Furthermore, the aggregation behavior of the complexes in both the pure solvent and the water/organic solvent were analyzed by electrical conductivity, NMR spectrometry, and vapor pressure depression (VPD).

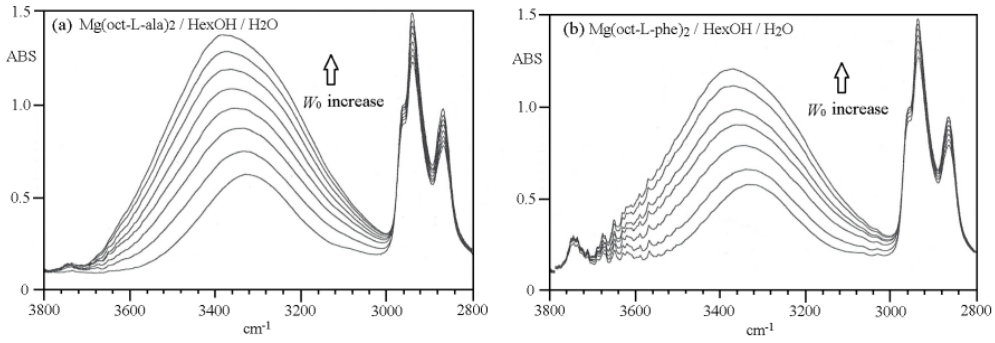

Fig.1 FT IR spectrum of the solvents and metal complex

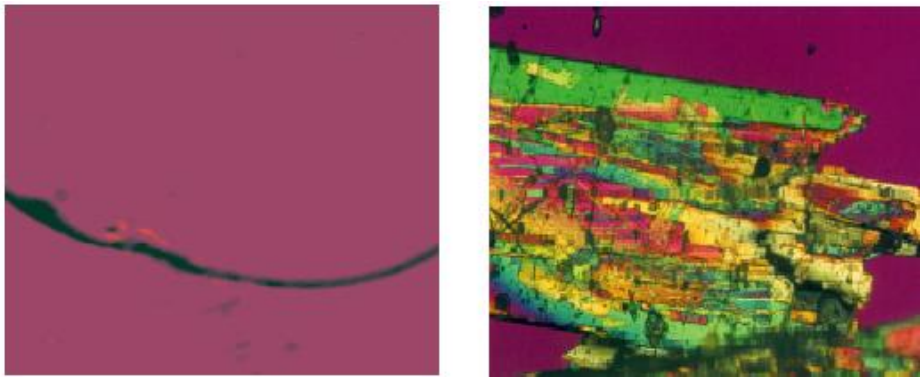

Fig.2 Polarized micrograph of metal complexes

Acknowledgements: This work is supported by the national natural science fund project (21663018), and the natural science fund project of Inner Mongolia (2018MS02011)

Structure and magnetocaloric effect of $Mn_{1.25}Fe_{0.75}P_{0.50}Si_{0.50}B_x$ alloys

Shouyuan Xing[1], Jiaying Zhang[1], Lin Song[1, 2], and Zhiqiang Ou[1, 2]

[1] *School of Physics and Electronic Information, Inner Mongolia Normal University, Inner Mongolia, Hohhot 010020, China;*

[2] *Inner Mongolia Key Laboratory for Physics and Chemistry of Functional Material, Inner Mongolia Normal University, Hohhot 010022, China*

Email: ouzhiqiang_nsd@hotmail.com

Abstract: Structural and magneto-caloric effect (MCE) of the $Mn_{1.25}Fe_{0.75}P_{0.50}Si_{0.50}B_x$ (x = 0.01, 0.02 and 0.04) alloys have been investigated. XRD result shows that the all the alloys crystallize in Fe_2P-type hexagonal structure with space group $P\bar{6}2m$. It is found that the lattice parameter a increases and the lattice parameter c slightly decreases with increasing x. The magnetic measurements show that the Curie temperature increases from 219 K to 323 K. The maximum magnetic entropy changes in a field change of 0 ~ 1.5 T are 6.1, 5.3 and 3.5 J/kg•K for x = 0.01, 0.02 and 0.04, respectively.

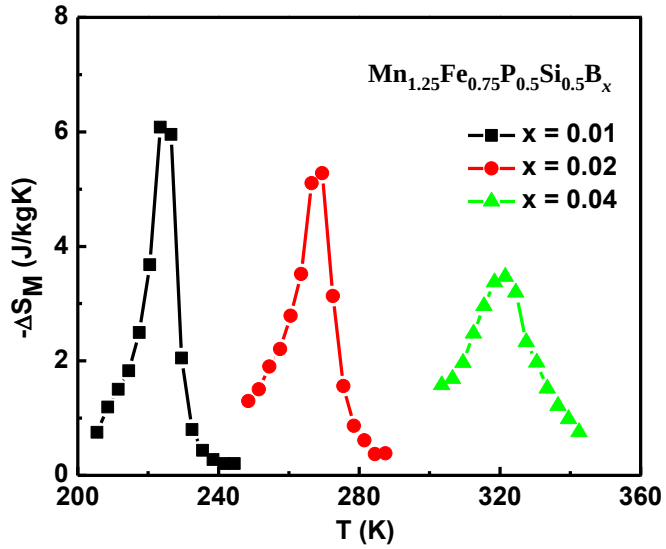

Fig. 1 Isothermal magnetic-entropy changes of $Mn_{1.25}Fe_{0.75}P_{0.5}Si_{0.5}B_x$ (x = 0.01, 0.02 and 0.04) alloys for an external field change of 0~1.5 T.

References

[1]. O. Tegus, E. Brück, K.H.J Buschow, F.R. de Boer, *Nature*, **415**, 150 (2002).

An Analysis of Some Bronzes Excavated from the Xindianzi Cemetery in Inner Mongolia

Song Zhiqiang[1], Sun Jinsong [1,2],Yong Mei[1],Cao Jianen[1,2], O Tegus[1, 3]

[1]*Institute for the History of Science and Technology,Inner Mongolia Normal University, Inner Mongolia, Hohhot 010020, China;*

[2] *Cultural Relics and Archeology Research Institute of Inner Mongolia, Inner Mongolia , Hohhot 010011, China ;*

[3] *Inner Mongolia Key Laboratory for Physics and Chemistry of Functional Materials, Inner Mongolia Normal University, Hohhot 010022, China*

Email: zhiqiangyouxiang@126.com

Abstract: The bronzes not only provide important materials for researching history, culture and art, but also provide important information about the relation of the materials preparation methods and their corrosion resistance. This paper presents the scientific examinations of some bronzes unearthed in Xindianzi cemetery in Inner Mongolia. The analysis results show that the bronzes contain mostly Cu-Sn-Pb alloys, which were mainly manufactured by casting. On the basis of the investigation, the technical features of the bronzes unearthed from Xindianzi cemetery are discussed. Historically, the results also provide scientific basis for the study of bronzes making technology in the central and southern region of Inner Mongolia.

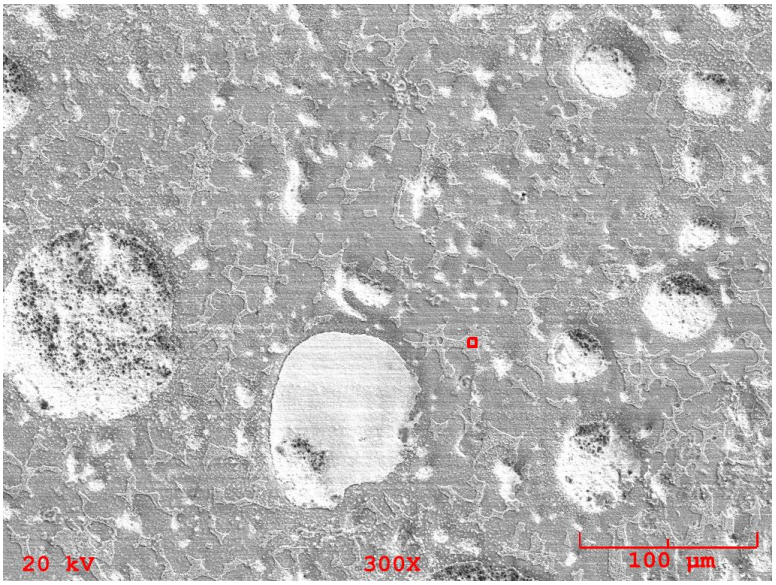

Fig.1. Scanning electron microscope image of the sample

References

[1]. G.Tian,*Steppe Cultural Relics*,**01**,1-20(1992).

[2]. J.Cao,*Archaeology*,**03**,195-206(2009).

Magnetostriction and microstructure of $Fe_{100-x}Al_x$ alloys

Rui Wang[1], Xiao Tian[1,*], Zhanquan Yao[2,*]

[1]*Inner Mongolia Key Laboratory for Physics and Chemistry of Functional Materials, School of Physics and Electronic Information, Inner Mongolia Normal University, Hohhot010022, China;*

2 School of Water Conservancy and Civil Engineering, Inner Mongolia Agricultural University, Hohhot 010018, People's Republic of China

Email:wangruiwr1110@163.com;nsdtx@imnu.edu.cn;ndyzq@imau.edu.cn

Abstract: In this work, the as-cast $Fe_{100-x}Al_x$ (x=17, 18, 19, 20) series alloys were prepared by vacuum arc-melting under argon atmosphere. The microstructures of the alloys were analyzed by X-ray diffractometer (XRD) and metallographic microscope (OM).

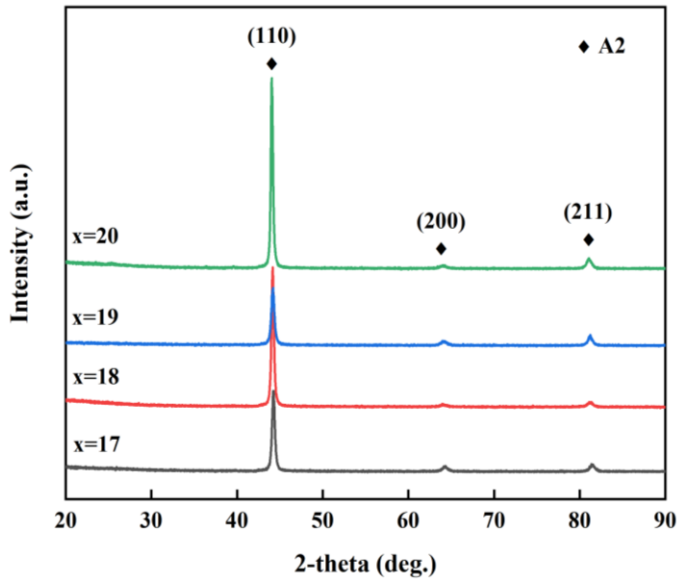

Fig.1 XRD patterns of $Fe_{100-x}Al_x$ alloys

The manetostriction cofficients of the $Fe_{100-x}Al_x$ alloys were measured by strain gauge method. The results show that all the alloys are composed of a single A2 phase with bcc structure, and the microstructures of this series of alloys are all

equiaxed crystals with coarse grains. The highest value of magnetostriction (52 ppm) has been found in the $Fe_{81}Al_{19}$ alloy, and the magnetostrictive coefficient of Fe-Al alloy can be compared with Fe-Ga alloy. The enhancement of magnetostriction of Fe-Al alloy is attribute to the preferred orientation of <100> direction.

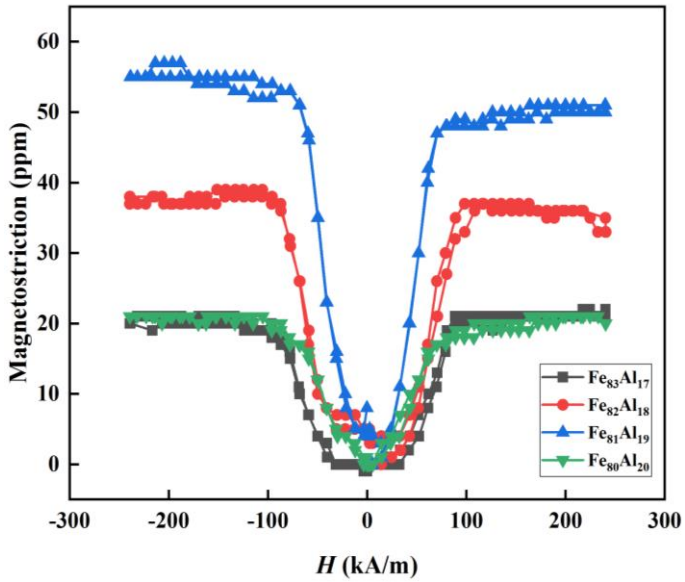

Fig.2 Magnetostriction of $Fe_{100-x}Al_x$ alloys versus applied magnetic field

Acknowledgements

This work is supported by the National Natural Science Foundation of China (51661027) and the Natural Science Foundation of Inner Mongolia (2019MS05002. 2020MS05075).

References

[1]. Z. H. Liu, G. D. Liu, M. Zhang, G. H. Wu, F. B. Meng, H. Y. Liu, L. Q. Yan, J. P. Qu, Y. X. Li. Large magnetostriction in $Fe_{100-x}Al_x$ ($15 \leqq x \geqq 30$) melt-spun ribbons. Applied Physics Letters. 2004, 85(10), 1751-1753.

[2]. N. Mehmood, R. Sato Turtelli, R. Grossinger, M. Kriegisch. Magnetostriction of polycrystalline $Fe_{100-x}Al_x$ (x =15, 19, 25). Journal of Magnetism and Magnetic Materials. 2010, 322, 1609-1612.

Preparation of the efficient Inverted Perovskite Solar cells with NiO as hole transport layer

Wenbing Meng [1], Yali Zhu [1], Xiaoyu Lv [2], Jun Ning[1, 2], Alata Hexig, Bingqin Zhou, Tegus[1, 2, 3]

[1]*College of Physics and Electron Information, Inner Mongolia Key Labteroary of Physics and Chemistry for Functional Materials*

[2] *Inner Mongolia Normal University*

Email: ningjun@imnu.edu.cn, zhoubq@imnu.edu.cn

Abstract: Inverted perovskite solar cells with NiO_x hole transport layer have attract the high attention because of the its low cost, high stability and easy fabrication. In this abstract, we used NiO_x film as the hole transport layer, PCBM film as the electron transport layer, $MAPbI_3$ film as the active layer of the perovskite solar cells, and investigated the influence of NiO_x, $MAPbI_3$ and PCBM film's preparation method on the photovoltaic performance of devices. It has been indicated that the morphology and thickness of the NiO_x hole transport layer, quality of perovskite film and PCBM film will affect the photovoltaic performance of the device[1],[2]. The results showed that the photovoltaic performances of perovskite solar cells enhanced obviously after the process optimization of NiO_x layer, perovskite layer and PCBM layer film. The maximum open circuit voltage(V_{oc}) and the highest power conversion efficiency(*PCE*) of device increased to 1.05 V and 13.75%, respectively.

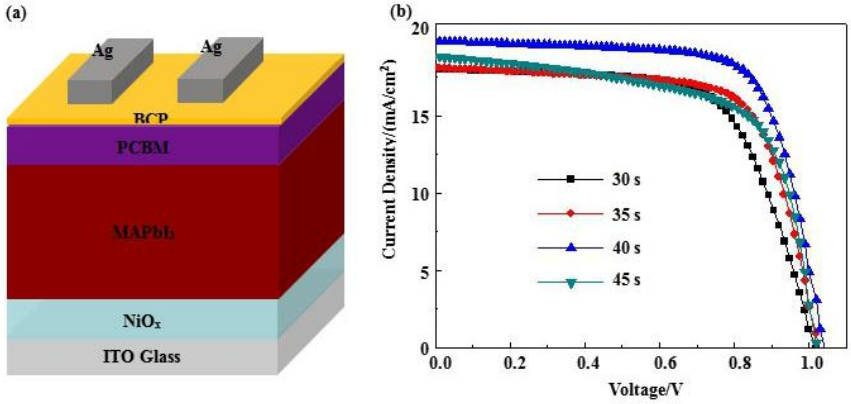

Fig.1 (a) Diagram of device structure; (b) *J-V* curves of perovskite solar cells for different injection timeing of anti-solvent toluene

References

[1]. X W Yin, Z B Yao, Q Luo, et al. ACS Appl. Mater. Interfaces, **9(3)**, 2439-2448(2017).

[2]. [2] F Huang, M Li. Energy Environ. Sci., **12(2)**, 518-549(2019).

Effects of different polar groups on the Liquid Crystal properties of the yttrium (III) Acyl –alaninate Complexes

Zhang Ying[1], Naren Gerile[1,2 *], Zhang Jinkang[1], Shi Yifeng[1], Alatan Bolag[1,2], O.Tegus[1,2]

[1]*College of Physics and Electronic Information, Inner Mongolia Normal University, Huhhot 010022, China*

[2]*Inner Mongolia Key Laboratory for Physics and Chemistry of Functional Materials, Inner Mongolia Normal University , Huhhot 010022, China*

email: naren88@hotmail.com

Abstract: Yttrium(Ⅲ) Acyl-alaninate complexes $Y(oct\text{-}ala)_3$,$Y(oct\text{-}phe)_3$,$Y(oct\text{-}ser)_3$) were prepared by chemical reaction method in methanol solution. These complexes were characterized by elemental analysis, UV-Vis, FT-IR, ^1H NMR, polarizing microscope and XRD. Element analysis and ^1H NMR suggest the complexes have a 1:3 stoichiometry. The chemical functional groups of the Y(Ⅲ) complexes were study by FT-IR. From the XRD and polarizing microscope studies, it has been concluded that Y(Ⅲ) complexes display transparent liquid crystal glass state.

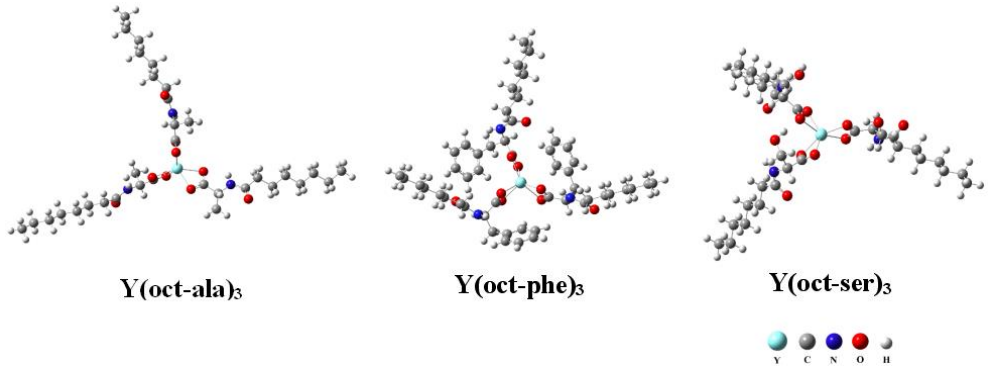

Fig. 1 (a) $Y(oct\text{-}ala)_3$; (b) $Y(oct\text{-}phe)_3$; (c) $Y(oct\text{-}ser)_3$ complexes.

Acknowledgements: This work is supported by the national natural science fund project (21663018), and the natural science fund project of Inner Mongolia (2018MS02011).

References

[1]. Gerile Naren,Tana Bao, Jun Ning, et al. Optical properties and aggregation behavior of environmentally friendly Lanthanum (III) acyl-alaninnate complexes[J]. *Arabian Journal of Chemistry*, 2020, 13(6): 5864-5877

[2]. Gerile Naren, Alata H, Tian Xiao, et al. Preparation and Characterization of Stable Molecular Glasses of Europium(III) Acyl-Alaninate complexes [J]. *Solid State Phenomena*, 2018, 271: 34-39.

Preparation and spectrial studies of silicon nitride thin films containing amorphous silicon quantum dots

Zhou Bingqing*, Gu Xin and Sun Jiaxin

Key Laboratory of Physics and Chemistry for Functional Material, College of Physics and Electron Information, Inner Mongolia Normal University, Huhhot 010022, China

Email: zhoubq@imnu.edu.cn

Abstract: Silicon-rich silicon nitride thin films were prepared on P-type monocrystalline silicon wafer (100) and glass substrate by plasma chemical vapor deposition with reaction gas sources SiH_4 and NH_3. As-deposited samples were thermally annealed from 600℃ to 1000℃ in a atmosphere furnace filled high purity nitrogen. The annealing time is 60 minutes. Fourier transform infrared spectroscopy (FTIR) was carried out to investigate the bonding configurations in the films. The results show that the Si-H bond and N-H bond decrease with the increase of annealing temperature, and completely disappear at the annealing temperature of 900℃. But the Si-N bond was enhanced with the increase of annealing temperature, and the blue shift occurred, and Si content in the film increased. The Raman scattering spectroscopy was used to study the phase structure of the samples, and confirm the presence of amorphous Si quantum dots (QDs). We found that the Raman peak of amorphous silicon appeared at 480cm^{-1} in the films at annealing temperature of 700℃. As shown in figure 1, the Raman peak after annealing at 1000℃ was fitted with two peaks, and the Raman peak of 497cm^{-1} crystalline small silicon particles was found, indicating that the silicon phase in the films changes

from amorphous to crystalline with the increase of annealing temperature. The experiment also through PL spectrum analyses the luminescence properties of the samples, found that there are five luminescence peaks in each sample under different annealing temperature. Based on the analysis of Raman spectrum and FTIR spectrum, the PL luminescence peak of amorphous silicon quantum dots appear at the wavelength range of 525-555nm, and the other four PL luminescence peaks are all from the defect state luminescence in the thin films, and according to the formula to calculate the amorphous silicon quantum dot size.

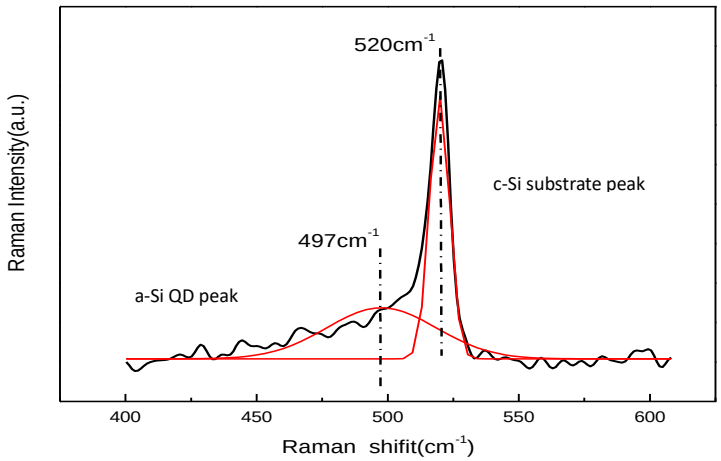

Fig.1 Raman spectrum of Si amorphous Si quantum dots in a SiN_x matrix

Reference

[1]. ZHANG Lin-rui, ZH0U Bing-qing, ZHANG Na, et al, Influence of Nitrogen Flow Rate on the Structure and Luminescence Properties of Silicon-Rich Silicon Nitride Film Materials in a High Hydrogen Atmosphere, *Spectroscopy and Spectral Analysis*, 2016,**30**(7):2049-2054.

[2]. Anthony R, Kortshagen U, Photoluminescence quantum yields of amorphous

and crystalline silicon nanoparticles . *Phys.Rev.B*,2009,**80**(11).

[3]. XIE Zheng-fang, SHAN Wen-guang, WU Xiao-shan et al., Effect of Annealing Temperature on Photoluminescence Performance and Structure of Si-rich Silicon Nitride,*Chinese Journal of Luminescence*, 2012,**33**(4):781-784.

[4]. Deshpandc S. V, Gulari E., Brown S. W, et al., Optical properties of silicon nitride films deposited by hot filament chemical vapor deposition, *Appl. Phys.*, 1995,**77**(12): 6534-6540.

[5]. Molinari M, Rinnert H,Vergnat M, Evolution with the annealing treatments of the photoluminescence mechanisms in a-SiNx: H alloys prepared by reactive evaporation, *Appl Phys*, 2007, **101** (12): 123532.

Synthesis of nitrogen-doped hierarchical porous carbon materials and its catalytic ability in hydrogen evolution reaction

Li Jinhao[1], Zhang wunengerile[1], Wu Yun[1], Muschin Tegshi[1], Jia Jingchun[1], Bao Agula[1]*

[1]*Inner Mongolia Key Laboratory of Green Catalysis, College of Chemistry and Environmental Science, Inner Mongolia Normal University, Hohhot 010022, Inner Mongolia, China*

Email: 546756039@qq.com

Abstract: In the current situation of sustained economic development and rapid population growth, it is people's desire to find a new type of sustainable energy sources[1]. Hydrogen energy is the best candidate for new energy because it has such advantages like abundant reserves, renewable and recyclable. Hydrolysis for hydrogen production is the most effective method. At present, the commonly used Pt based noble metal catalysts have relatively good catalytic performance, but their scarcity and high price limit their large-scale application[2]. Therefore, people urgently need to find cheap and efficient metal-free electrocatalysts to replace the noble-metal electrocatalysts in the HER reaction. In this paper, N-doped hierarchical porous carbon materials were fabricated via template-free method. The catalysts were characterized by XRD, N_2-adsorption desorption, TEM, Raman, FT-IR, and so on. After that, we studied the effects of different nitrogen sources and different carbon sources on the HER performance of porous carbon materials. The result indicated the ethylene-diamine based porous carbon material (NPC-2) compared with other nonmetallic heteroatom (N, F, B, S) doped carbon materials and some traditional metallic catalysts exhibited excellent HER performance and stability in 0.5 M H_2SO_4. To achieve a 10 mA/cm^2 HER current density, the nitrogen-doped hierarchical porous carbon materials (NPC-2) required an overpotential of 398 mV. This is because the heteroatom

could activate the adjacent C atom in the porous carbon materials by affecting its valence orbital energy levels to improve HER performance.

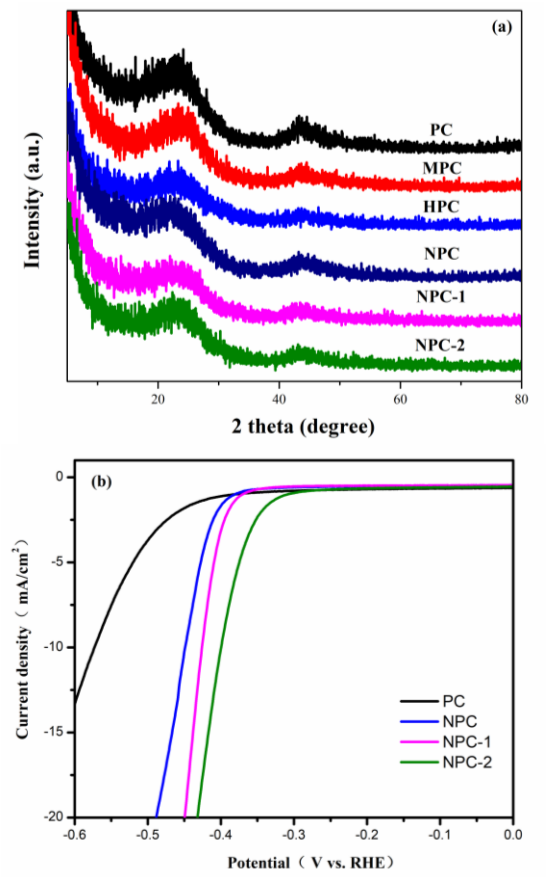

Fig.1. (a) XRD patterns of all samples and (b) Polarization cures of the porous carbon material synthesized by different carbon sources in 0.5 M H_2SO_4.

Acknowledgments

The paper is supported by the Collaborative Innovation Center for Water Environmental Security of Inner Mongolia Autonomous Region, China (XTCX003)

References

[1]. Z. Pu, Q Liu, M. Asiri, et al. *Electrochim Acta*, **168**, 133-138 (2015).

[2]. F. Yu, H. Zhou, F. Huang, et al. *Nat Commun*, **9**, 2551-2560 (2018).

Magnetic Properties of $MnFe_{0.6}Ni_{0.4}Si_{1-x}Al_x$ Alloys

Nuendute[1,2], Ou Zhiqiang[1,2], H. Yibole[1,2],

Siqin Bator[1,2], O. Tegus[1,2]

[1]*Inner Mongolia Key Laboratory for Physics and Chemistry of Functional Materials, Inner Mongolia Normal University, Hohhot 010022, China*

[2]*College of Physics and Electronic Information, Inner Mongolia Normal University, Hohhot 010022, China*

Email: tegusph@imnu.edu.cn

Abstract. Mn*MX* manganese alloys where *M* is a 3*d* transition metal and *X* a metalloid or a non metal form a rich material families with intriguing physics in general and magnetism in particular. In recent years, Mn*MX* alloys showing such simultaneous structural orthorhombic TiNiSi to the hexagonal Ni_2In and magnetic transitions have been most active as the associated large volume change and latent heat result in giant negative thermal expansion and magnetocaloric effect. This paper meanly focus on the structural and magnetic properties of $MnFe_{0.6}Ni_{0.4}Si_{1-x}Al_x$ alloys (x = 0.02, 0.04, 0.06, 0.08) are explored using powder X ray diffraction and magnetic measurements, the crystal structure evolves from the orthorhombic TiNiSi type to the hexagonal Ni_2In type (see Fig. 1) with the increase of Al contents and a magneto structural coupling leading to a first order ferromagnetic transition is found at 284 K for x = 0.06 (see Fig. 2). In addition, the magnetocaloric effects in this alloy system were determined on the basis of isothermal magnetization mearsurements. Therefore, this research is of great significance for exploring new type of room temperature magnetic refrigeration materials.

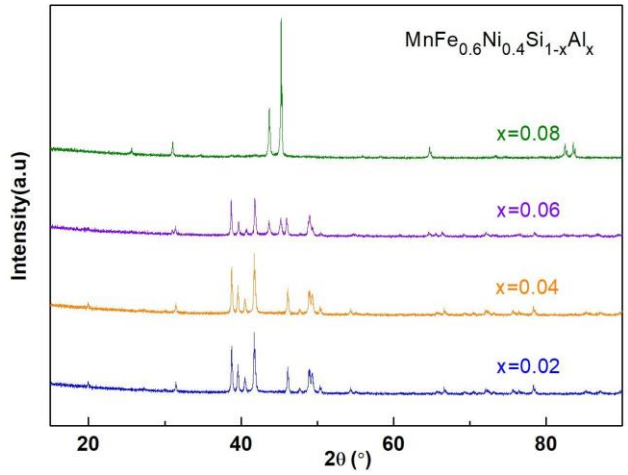

Fig.1 XRD patterns of the samples

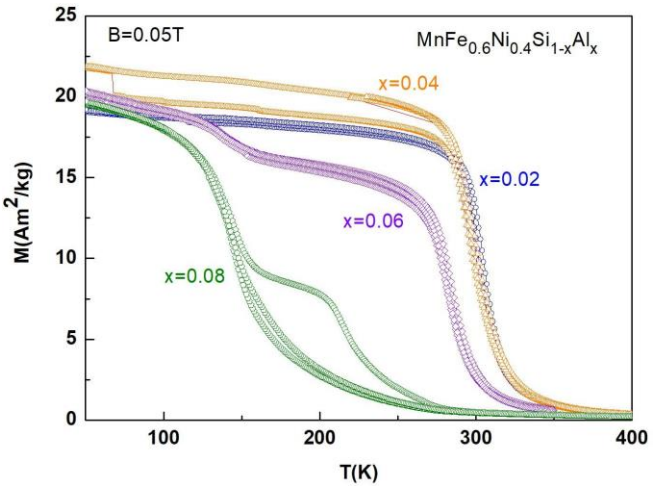

Fig.2 *M-T* curves of the samples

Reference

[1]. W. Hanggai, O.Tegus, H. Yibole, F. Guillou Structural and magnetic phase diagrams of MnFe0.6Ni0.4(Si,Ge) alloys and their giant magnetocaloric effect probed by heat capacity measurements, Journal of Magnetism and Magnetic Materials, **49415**, 165785,2020.

Receiving, Modeling of Formation, Properties of Composite Metal/Semiconductor Nanoparticles

A.V. Nomoev[1,2], N.V. Yumozhapova[1,2], E.Ch. Khartaeva[1]

[1]*Institute of Physical Materials Science, Siberian Branch of the Russian Academy of Sciences, Sakhyanovoy st., 6, Ulan-Ude, 670047, Russia*

[2]*Buryat State University, 24a Smolin st. Ulan-Ude, 670000, Russia*

e-mail: nomoevav@mail.ru

Interest in the study of composite nanoparticles – core/shell and Janus like is due to the following reasons. Unique properties of core-shell nanoparticles: preservation of core from oxidation and others impacts, changing magnetic (magnetization), optical (luminescence, absorption) properties due to interaction between core and shell. Core/shell nanoparticles reduce the size of nanoparticles and agglomeration of nanoparticles, which prevents the appearance of nanoscale properties of powders. Presence of plasmon resonance in the visible region of the spectrum [1,2]. Core-shell nanoparticles are precursors for the synthesis of 0 D nanoparticles of the second and third generations and amplificate the luminescence. Reduction of the thermal conductivity of hollow nanoparticles. Composite nanoparticles increase magnetic properties. Interesting properties of Janus-like nanoparticle – charge separation. As result of separation is big dipole moment. Janus nanoparticles metal/semiconducor have Schottky contact [2]. That property gives opportunity increase effective operation of them by electrical fields.

Nanoparticles are created in a single-step way. We received copper and composite nanoparticles (core-shell, Janus-like, hollow) by two methods using electron beam and laser irradiation. A high-performance method for evaporation of matter by a relativistic electron beam followed by condensation of vapors in an inert gas stream – prof. Bardakhanov method [3]. The electron energy was 1.4 MeV, the beam current was varied from 3 to 10 mA, spot area was 7 cm2 and the maximum power density was 106 W/cm2. The temperature of the effective

radiation spot is Te = 5000°C. Second method: Laser ablation. Laser Power is 100 W. Impulse duration is varied from 10 ns to 100 ns.

According to our assumption the main reason for creating a core-shell nanoparticle is the difference between the surface energy of the two components of this compound. When the core has a greater surface energy than the surface energy of the shell, the core-shell particle has a minimum total energy. However, when cooling velocity is a quick we can see creation of Janus like nanoparticle. The electron beam irradiates two substances, the vapors from the surface of the substance are cooled by the transport gas argon. A drop of liquid of two substances will form. When the surface energies of two substances are different, core-shell nanoparticles are formed. If the values of surface energies are equal, core-shell nanoparticles will form if the vapor concentration of one substance is much higher than that of the second. Small particles condense into large ones. When substances create chemical bonds, Janus-type nanoparticles are formed.

The size distribution of nanoparticles is determined by the dynamic scattering of laser light. The distribution of scattered laser light from nanoparticles depends on their size. Backscattered light intensity decreases with increasing particle size. This pattern allows us to determine their size. The size distribution of nanoparticles created by the gas-phase condensation method usually corresponds to the log-normal. The equation is called the Smoluchowski kinetic equation and describes the evolution of the distribution function of particles in time through their coagulation. The main conditions under which this equation makes sense can be formulated as follows: - the disperse system is so rarefied that only pair interactions of particles can be considered, and triple interactions, etc. can be neglected - there is an element of randomness in the dispersed system, so the behavior particles between acts of coagulation are not statistically dependent. However, the size distribution of composite nanoparticles created by the gas-phase condensation method does not correspond to the logarithmically normal one. The size distribution of Janus-like Ag/Si nanoparticles is closer to normal. The size distribution of copper /silicon nanoparticles core/shell differs from lognormal. The main reason for these differences is in the different mechanisms of creation.

It is known that a Schottky contact is created when a metal is combined with a semiconductor. The Janus-like TaSi2/Si nanoparticle is a Schottky contact, because Si is a semiconductor, and TaSi2 is a conducting material. We measured the volt-ampere characteristics by the AFM method and found that the contact is ohmic, that means the metal/ semiconductor contact conduct electrical current at forward (positive) and opposite (negative) bias voltage. Usually, when contact is big and has micrometer size, TaSi2/Si has ohmic contact. In order to will make nonohmic nanocontact with diode characteristic we will use another nanoparticle Ag/Si. This microsize contact has diode characteristic and we hope that nanosize Ag/Si contact wil have nonohmic contact.

At a concentration of dopants of 10^20 cm-3, the ideality coefficient is 1.7, which means that the system deviates significantly from the ideal behavior of the Schottky diode. This can be explained by the fact that at such concentration silicon becomes a degenerate semiconductor. In the future, it is planned to reduce the concentration of alloying substances to reduce the influence of the electrical properties of the impurity.

References

[1]. A.V. Nomoev, S.P. Bardakhanov, M. Schreiber, D.Zh. Bazarova, B.B. Baldanov, N.A. Romanov, Synthesis, characterization, and mechanism of formation of Janus-like nanoparticles of tantalum silicide-silicon (TaSi2/Si), Nanomaterials. 2015. T. 5. № 1. 26-35. doi: 10.3390/nano5010026

[2]. Nomoev A.V., Torhov N.T., Khartaeva E.Ch., Syzranthev V.V., Yumozhapova N.V., Tsyrenova M.A., Mankhirov V.N., Special aspects of the thermodynamics of formation and polarization of Ag/Si nanoparticles, Chemical Physics Letters. 2019. Vol. 720. pp 113-118. https://doi.org/10.1016/j.cplett.2019.02.015

[3]. S.P. Bardakhanov, A.I. Korchagin, N.K. Kuksanov, A.V. Lavrukhin, R.A. Salimov, S.N. Fadeev, V.V. Cherepkov, Nanopowders obtained by evaporating initial substances in an electron accelerator at atmospheric pressure, Dokl. Phys. 51 (7) (2006) 353–356, https://doi.org/10.1134/S1028335806070044.

Aggregations of Fullerenes (C_{60}) in Water and NMP: A Molecular Dynamic Study

M.Chagdarjav[1], N.Jargalan[2], B.Batgerel[1], B.Mijiddorj[3]

[1]*Institute of Mathematics and Digital Technology, Mongolian Academy of Sciences, Ulaanbaatar 13330, Mongolia*

[2]*Institute Physics and Technology, Mongolian Academy of Sciences, Ulaanbaatar 13330, Mongolia*

[3]*School of Engineering and Applied Sciences, National University of Mongolia, Ulaanbaatar 14201, Mongolia*

Abstract: Fullerene family molecules, one of the allotropic form of carbon, have received significant attention due to their wide range of structural and functional capabilities. Fullerenes show similar physical properties to graphene and carbon nanotubes and dissolve in a wide variety of solvents. This advantage attracts the attention of biologists and medical scientists because fullerenes are organic molecules. The properties of fullerenes in solution have been studied since the early 1990s. Depending on the properties of the solvent, the fullerene showed interesting phenomena such as nonlinear dissolution, solvatochromic effect, and cluster growth in different solutions [1-4]. The most interesting phenomenon is cluster growth in solvents. The formation of fullerene clusters in solution consists of two main mechanisms: the fullerene-fullerene and fullerene-solvent molecules through bonding [5]. The experimental studies observed that a complex formation of fullerene with some polar solvents (like as donor-acceptor) such as C_{60}/NMP, C_{60}/Pyridine. The fullerene clusters are observed up to ~500 nm and more stable in polar solutions [6]. However, it has not yet fully understood that how they aggregate the fullerene-fullerene and the fullerene-solvent at the molecule level.

In this work, we applied molecular dynamic simulations to observe the aggregation of fullerenes in water and NMP solutions.

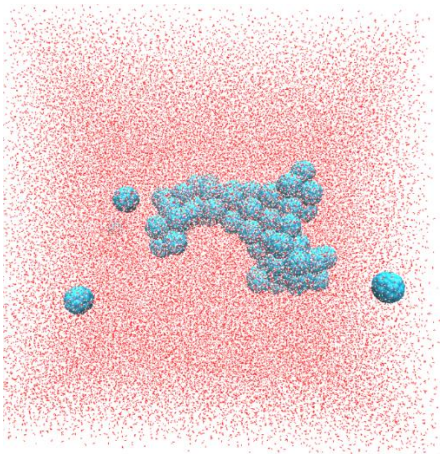

Figure. C_{60}/Water system after MD simulation

References

[1]. R.S. Ruoff, S.T. Doris, R. Malhotra, D.C. Lorents. Solubility of fullerene (C_{60}) in a variety of solvents. J. Phys. Chem. 97, 3379 (1993).

[2]. R.S. Ruoff, R. Malhotra, D.L. Huestis, D.S. Tse, D.C. Lorents. Anomalous solubility behaviour of C_{60}. Nature 362, 140 (1993).

[3]. N. Jargalan, T.V. Tropin, M.V. Avdeev, V.L. Aksenov, "Investigation of dissolution kinetics for fullerene C60 in toluene, benzene and NMP solvents", Proceeding of Institute of Physics and Technology, Vol 40, pp. 15-18, 2013.

[4]. T.V. Tropin, M.V. Avdeev, N. Jargalan, M.O. Kuzmenko, V.L. Aksenov, "Kinetics of cluster growth in fullerene solutions of different polarity", Springer proceedings in physics book series, vol 223 (2019), 249-272

[5]. T.V. Tropin, N. Jargalan, M.V. Avdeev, O.A. Kyzyma, R.A. Eremin, D. Sangaa, V.L. Aksenov. "Kinetics of cluster growth in polar solutions of fullerene: Experimental and theoretical study of C60/NMP solution", Journal of Molecular Liquids, vol 175, pp. 4–11, 2012

[6]. T. V. Tropin, M. V. Avdeev, O. A. Kyzyma, R. A. Yeremin, N. Jargalan, M. V. Korobov, V. L. Aksenov, "Towards description of kinetics of dissolution and cluster growth in C60/NMP solutions", Physica Status Solidi B, Vol 248, pp. 2728–2731, 2011.

Biocompatibility of $Mg_{0.8}Ni_{0.2}Fe_2O_4$ ferrite nanoparticles evaluated by in vitro cytotoxicity assays using HeLa cells

I.Khishigdemberel[*1], N.Nomin[2], Gantulga[2], E. Uyanga[1], B. Enkhmend[1], Ts.Oyunsuren and D.Sangaa[1]

[1]*Institute of Physics and Technology, Mongolian Academy of Sciences, 13330 Ulaanbaatar, Mongolia*

[2]*Institute of Biology, Mongolian Academy of Sciences, 13330 Ulaanbaatar, Mongolia*

**E-mail: khishigdembereli@mas.ac.mn*

Abstract: Magnetic nanoparticles for thermo therapy must be biocompatible and possess high thermal efficiency as heating elements. The biocompatibility of $Mg_{0.8}Ni_{0.2}Fe_2O_4$ nanoparticles was studied using a cytotoxicity colony formation assay and a cell viability assay. HeLa cells exhibited cytotoxic effects when exposed to concentrations of 50μg/ml nanoparticles. In vitro cytotoxicity of samples was then investigated by two methods, colony formation assay and cell viability assay. The colony formation assay is a commonly used assay to evaluate the cellular proliferative potential and is widely used in the field of radiation biochemistry [1], chemotherapy and toxicology [2].

In these experiments, cultured cells were exposed to magnetic nanoparticles, and the number of colonies which adhered normally to culture vessels evaluated. The ratio of colonies was defined as the number of colonies counted seven days after exposing the cells to magnetic nanoparticles compared with the number of colonies counted with no added nanoparticles.

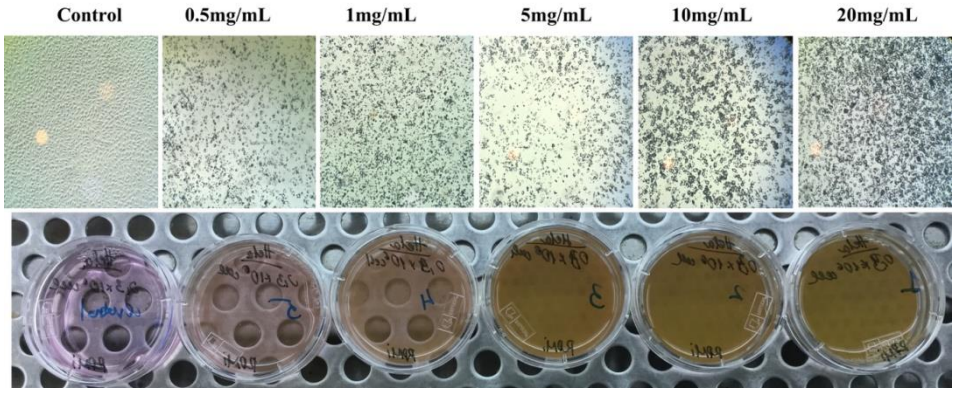

Figure 1. Images of the cultured cells with magnetic nanoparticles after 24h (20x)

Reference

[1]. T. Saga, H. Sakahara, Y. Nakamoto, et al., Eur. J. Cancer 37 (2001) 1429.

[2]. J. Jimenez, L.R. Negrete, F. Abdullaev, et al., Exp. Toxicol. Pathol. 60 (2008)

Antioxidant activity of blueberry peel

B. Khongor*, B. Davaasuren, R. Khoroljav, D. Naidan, J. Erdenetogtokh
Institute of Physics and Technology, Mongolian Academy of Sciences
*bhongor7@gmail.com

Abstract: 10000-20000 free radicals are formed in the average human body each day due to the caloric effects of human nutrition and the effects of environmental factors such as UV radiation, air pollution, smoking, and alcohol. Since free radicals are highly reactive molecules or atoms containing unpaired electrons in their orbitals, they can bind to and damage healthy molecules that make up the body. This damages body tissues, cells and organs, and causes aging. It is also a major cause of deadly diseases like cancer and cardiovascular diseases. This is the reason for research into antioxidants that scavenge free radicals. In this study, the antioxidant activity of blueberry juice extracted from blueberry peel at the Teso LLC plant was investigated. It is very important and useful to study and introduce the antioxidant activity of national industrial products, as our country not only has the world's leading cancer rate, but also the average life expectancy is lower than the world average. In the beginning, the antioxidant activity of the pure juice was measured by using photochemiluminescence method, and very high activity was detected that was well above the measuring range of the photochemiluminometer. However, when the juice was diluted 200 times, the activity was almost equal to that of the dimethyl sulfoxide.

Keywords:Antioxidant activity, blueberry, dimethyl sulfoxide, photochemiluminescence

Study on catalytic activity of citrate-stabilized silver nanoparticles

Bayasgalan Ulambayar[1], Nomin-Erdene Battulga[1], Ikhbayar Batsukh[2], Khaliun Nomin-Erdene[1], Ninjbadgar Tsedev[3], Rentsenmyadag Dashzeveg[1], Galbadrakh Ragchaa[4], Erdene-Ochir Ganbold[4,*]

[1]*Department of Chemistry, School of Arts and Sciences, National University of Mongolia, Mongolia*

[2]*Department of Chemical and Biological Engineering, School of Engineering and Applied Sciences, National University of Mongolia.*

[3]*Center for Advanced Materials, National University of Mongolia*

[4]*Department of Physics, School of Arts and Sciences, National University of Mongolia, Mongolia*

**corresponding author: erdeneochir_g@num.edu.mn*

Abstract: Colloidal dispersions of spherical silver nanoparticles (AgNPs) have been synthesized by a citrate reduction method in which sodium citrate is utilized as both of reducing and stabilizing agents. Catalytic properties of as-synthesized AgNPs were examined using the reduction of 2,4-dinitrophenol (2,4-DNP) by sodium-borohydride. Experimental results revealed that the citrate-stabilized AgNPs is a very efficient catalysts for the degradation of 2,4-DNP.

Synthesis of Fe_2Co/Al_2O_3 by the Pechini method for use as catalyst in CNT preparation

Enkhtur Sukhbaatar[1], Tsog-Ochir Tsendsuren[2], Galbadrakh Ragchaa[1], Bayasgalan Ulambayar[3], Nomin-Erdene Battulga[3], Rentsenmyadag Dashzeveg[3], Erdene-Ochir Ganbold[1,*]

[1]*Department of Physics, School of Arts and Sciences, National University of Mongolia, Mongolia*

[2]*Institute of Physics and Technology, Mongolian Academy of Science*

[3]*Department of Chemistry, School of Arts and Sciences, National University of Mongolia, Mongolia*

*corresponding author: erdeneochir_g@num.edu.mn

Abstract: Alumina-supported Fe_2Co catalyst was synthesized by the Pechini method in which Fe as the core catalyst, Co as the co-catalyst, and Al_2O_3 as the catalyst carrier. To prepare catalysts, appropriate amount of ferric nitrate, cobalt nitrate and aluminum nitrate were dissolved under vigorous stirring in a solution containing ethylene glycol and citric acid at 95°C. Then, the sample went under heat treatment at various temperature after complete evaporation of solute molecules. Here, we prepared four different catalyst samples depending on the temperature of heat treatment in order to determine an optimal conditions to synthesize metal catalysts for carbon nanotubes via CVD method.

Solubility of Baganuur coal in imidazolium based ionic liquid as ([Bmim]Cl) by FTIR spectroscopic study

S. Munkhtsetseg[1], G.Erdene-Ochir[1], R.Galbadrakh[1], S.Enkhtur[1], A.N.Oleshkevich[2], N. M. Lapchuk

[1]*National University of Mongolia, Ulaanbaatar, Mongolia*

[2]*Department of Physics, Belarusian State University, Minsk, Belarus*

Abstract: In the present work, the extraction of Mongolian Baganuur coal in solvents as pyridine and ionic liquid with 1-butyl-3-methyl-imidazolium chloride ([Bmim]Cl) anion was first applied. The parent coal, its extracts and insoluble residues were then characterized using the Fourier transform infrared (FTIR) spectroscopy.

The obtained FTIR spectra have revealed many new features that were not observed before. An appearance or sharpening of the particular bands after the chemical treatment allow a determination of inactive or weak fundamental vibrations precisely. The received spectral results will be useful for the further Mongolian coal study as well as coal upgrading processes as a reference information.

Keywords: coal, pyridine, ionic liquid, FTIR

Mechanical and optical properties of fullerene contained polymers

E. M. Spilevski[1], S. A. Filatov[1], A. D. Zamkovets[2], G. Shilagardi[3], D. Ulam-Orgikh[3], S.Munkhtsetseg, P. Tuvshintur[3], D. Tumurbaatar[3]

[1]The A.V. Luikov Heat and Mass Transfer Institute of NAS of Belarus, Minsk, Belarus

[2] State Scientific Institution, B. I. Stepanov Institute of Physics of the NAS of Belarus, Minsk, Belarus

[3]National University of Mongolia, Ulaanbaatar, Mongolia

Abstract: Fullerenes own electric acceptor property based on that the non-covalence compounds of donor-acceptor types are formed by low molecular compounds. And such molecules have self-complex formation property that hold in the addition of various constructional and structural organizations to the polymers [1, 2]. In the current work it is presented results of the study for mechanical and optical properties to discover characteristics of interaction between components of polymer compositions that becomes the cause of development of polymers property. As a matrix for the inputting to the various concentration of fullerenes and their complexes with metals it is chosen widely used polymers as polystyrenes, polypropylene, and polyethylene under high pressure.

It is established that doping polymers to fullerenes and their complexes with metals leads to the change in mechanical and optical properties of the material. Properties of composites depend on portions containment of fullerenes and technological conditions of preparation. Fullerenes that doped into the matrix of polymers interact with molecular chains till its concentration equals 0.5 % C_{60} arranging matrix structure. Above this value of the percent, the concentration of C_{60} molecules segregate and form fullerites clusters whose size becomes bigger in the increase of the concentration. Therefore, structural processing passes through the arrangement of the polymers matrix structure under the small amount of concentration (up to 0.5-0.6 mass.% C_{60}), and contrary, in the formation and increase of fullerites clusters it is observed disordering.

It is presented metal-fullerenes nano-structures, those of on the surface of polymers, generate surface resonance plasma absorption. The plasma absorption corresponds to the maximum peak and its form and width of bands attribute to the mass portion of components, size of isles, degree of surface substrate filling, interior mechanical tension, condition on the border of metal and fullerite. This wide range of property opens a possibility of their applications. The presence of fullerens in the nano-structure leads weakening of collective electrodynamics interactions between metals nano-particles.

Properties of polymers in significant level depend on the portion containment of fullerenes. In the field of low concentration doping, their action results interaction of C_{60} molecule with polymer molecules following an increase of effectiveness density of polymers lattice. Macromolecular polymers and C_{60} bonding can be seen as additional nodes of spatial structural lattice. This additional structure determines mechanical properties of polymer systems of C_{60}. Molecule C_{60} influence to the conditions of the supramolecular structural formation of matrix, changing state of polymers.

[1]. Badamshina E, Gafurova M., Figovsky O., Shapovalov H. Fullerene-containing polyurethanes: review. J. Scientific Israel-Technological Advantages. 2006. V. 8. № 1, 2. P. 149-159.

[2]. E.M. Spilevski, G. Shilagardi, G. S. Akhremkova Mechanical and tribological properties of polyethelenes under high pressure modified as fullerenes // Fullerenes and fullerenes like structures. The A.V. Luikov Heat and Mass Transfer Institute of NAS of Belarus, Minsk, Belarus, 2005. P. 218-228.

Electrical properties of titanium-fullerene films

P.Tuvshintur[1], D.Ulam-Orgikh[1], M.Otgonbaatar[1], S.Munkhtsetseg[1], E.M. Shpilevsky[2], G.Shilagardi[1]

[1]*National University of Mongolia, Ulaanbaatar,15141, Mongolia,*

tuvshintur@num.edu.mn

[2]*Heat and Mass transfer Institute, NAS of Belarus, Minsk, Belarus,*

eshpilevsky@rambler.ru

Abstract

Abstract: The structure of films and coatings obtained by condensation of titanium atoms and C60-fullerene molecules from combined flows of these atoms and molecules in a vacuum and the electrical properties of the indicated films and coatings were investigated. It was established that the introduction of fullerenes into metal films and coatings substantially changes their structure and the electrical characteristics. It is shown that composite film structures of Ti-C60 in certain intervals of share composition components have properties R-C-L- circuit.

Results of research on discharge products

J.Vanchinkhuu[1], B.Duurenbuyan[2], M.Anand[1], E.Bayanjargal[3]

[1]*Department of Physics, School of Science, National University of Mongolia*

[2]*Laboratory of Biophysics, Division of Material Science, Institute of Physics and Technology, Mongolian Academy of Science*

[3]*Analitycal laboratory, Division of Material Science, Institute of Physics and Technology, Mongolian Academy of Science*

j.vanchinkhuu@num.edu.mn

Abstract: Products from arc discharge between various conducting materials (copper-copper, aluminum-aluminum, graphite-graphite, natural graphite and their cross combination) in water and air have been studied. The SEM and SEM EDS analysis of products from metallic electrodes was done as well their size distribution. There are two essential types of product taken in investigation as (i) pure metallic particulates, and (ii) specific structures of materials. The nano-sized products taken in two media at different current are compared [1,2]. In products obtained in air, tiny spherical particulates of size in nano-order are observed repeatedly, as well ordinary nanosized particulates as ones in water. The main visual feature of the particulates in air is their existence in deposition in which they are separated by itself. The individual scrolling sheets of graphite encounter in soot on electrodes. Main characteristics of products were determined.

Keywords: discharge in water and air, soot, ash, individual sheet of layer, shape of particulates, size distribution, particulate analysis.

References

[1]. J.Vanchinkhuu et al., (2017). Solid State Phenomena, Vol. 288, pp 71-78.

[2]. F.Liu, et al., (2010). Morphology Study by Using Scanning Electron Microscopy. Microscopy: Science, Technology, Applications and Education.

Dielectrophoretic force application in separating powder materials

J.Vanchinkhuu[1], J.Erdenetogtokh[2], B.Duurenbuyan[2], B.Anand[1]

[1]*Department of Physics, School of Science, National University of Mongolia*

[2]*Biophysics laboratory, Division of Material Science, Institute of Physics and Technology, Mongolian Academy of Science*

j.vanchinkhuu@num.edu.mn

Abstract: One of the ways producing long carbon nanotubes, nanowires and nanorods is the arc discharge in water and their electrode evaporation. In this process, nano- and micro sized particulates are produced and got into surrounding water. In practice, these particulates are taken in study by floating separation and drying methods. However, this is not the only way to separate the particulates in the water, discharge was maintained [1,2]. One can use the electrophoresis and electrokinetics in separation and fractioning of particulates. The materials, formed from arc discharge between graphite electrodes, are in powder form as well it is grown on electrode. Either form of products contains micro or nano sized particulates, the linear size of which ranges 16-1600nm, in various shapes [3]. Most of these particulates are in elongated form and this feature is the key factor for separation of particulates in size because the electrical multipole momentum of conducting ellipsoid dielectric particulates depends on its shape and size. The elongated particulates can be treated in calculation as ellipsoid in shape. When non-conducting particulates in dielectric medium are in an electric field, a dielectrophoretic force acts on the particulates. As for conducting particulates in electrical field, the force acting on them tends to deform their shapes. When the particulates are charged they are under the electrophoretic force. There are several mechanisms for charging of particulates in discharge region. We have considered separation and fractioning of particulates (i) departing the discharge region, (ii) formed on electrode by using electrophoretic actions.

References

[1]. Sandor B, Advances in Colloid and Interface Science, vol. 147–148, pp 36–43, 2009.

[2]. Bashar Y, Sensors, vol. 14, pp 6356-6369, 2014.

[3]. Vanchinkhuu J, et al., Solid State Phenomena, vol. 288, pp 71-78, 2018.

Method for decreasing erosion of technical tools in a condition of dry and friction

Oidov Jamyan[1], Purevjal Bayasgalan[1]

[1]*Railway Institute, Mongolia*

Email: ojamyan@gmail.com

Abstract: Various depreciations are still exist in all technical area. Technical tools and their components which are in a dry and frictioned conditions are affected considerably by erosion and their size and shapes are changed irreversibly.

Purpose of this work is to do experimental work to produce an alloy with hard-soft phase by wear-resistant coating of white cast iron on steel component and use it to practical applications. A white cast iron surface is created on a steel component by chemicothermo treatment. Caulking nozzle of a caulker train ВПРС-02 is used for the experiment. We created white cast iron surface on the nozzle. Then erosion of the nozzle decreased noticeably when it is used in working field.

Electrophysical properties of Janus-like silver nanoparticles

T.A. Chimytov[1,2], A.V. Nomoev[1,2]

[1]*Institute of Physical Materials Science, Siberian Branch of the Russian Academy of Sciences, 6, Sakhyanovoy st.,Ulan-Ude, 670047, Russia*

[2]*Buryat State University, 24a Smolin st. Ulan-Ude, 670000, Russia*

e-mail: nomoevav@mail.ru

Abstract: *The article presents the results of an experimental study of the electrophysical properties of Janus-like silver nanoparticles Ag/Si. The distribution of the electric potential of silver nanoparticles was obtained using atomic force microscopy using the Kelvin probe method. The electrical capacity of the particles is estimated.*

Recently, in connection with the development of nanoelectronic technologies, there is a great interest in Janus-like nanoparticles. The presence of an intrinsic dipole moment and electrical capacity of such particles provides additional opportunities for increasing the efficiency of the interaction of a particle with external electric and alternating magnetic fields.

In the current paper, we study particles of Ag/Si nanopowder obtained using gas-phase synthesis [1]. The nanopowder comprises agglomerates of various sizes (Fig. 1), which are interconnected particles of silver and silicon. In fig. 1 on the left, it can be seen that the agglomerates under study comprise spherical particles (about 100 nm). Elemental analysis indicates that the largest proportion of silicon falls on the substrate (comprising silicon) and decreases in the agglomerate's bulk (Fig. 1 - in the middle). On the right in Fig. 1 - distribution density of silver, which is maximum in the agglomerates themselves. The different chemical nature of these elements leads to the formation of a Schottky barrier and the separation of electric charges within the particle itself, which leads to the appearance of a dipole moment. The work [2] provides an estimate of the dipole moment – about $1{,}05 \cdot 10^{-29}$ C·m.

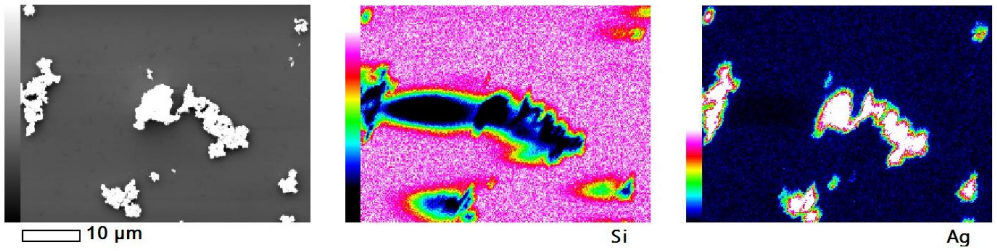

Fig. 1. The chemical composition of agglomerates of Ag/Si nanoparticles, determined using a scanning electron microscope NEOSCOPE II JCM-6000

The electric potential difference of Ag/Si nanoparticles was measured using a SolverNext atomic force microscope (AFM) (NT-MDT, Russia). To study the contact potential difference of the particles, we used a HA_NC cantilever (TipsNano, Russia), with which samples were scanned in the semi-contact mode (using the Kelvin probe method). The sample was a silicon substrate with particles of Ag/Si nanopowder deposited on it. Before preparing the samples, agglomerates of Ag/Si nanopowder particles were broken up by ultrasonic dispersion, by the method of acoustic cavitation in 99.7% isopropyl alcohol. For this, a cuvette containing a mixture of isopropyl alcohol and Ag/Si nanoparticles (mass fraction of powder - 0.5%) was placed in a 50 W ultrasonic bath for 10 minutes. After that, the mixture was settled for 15–20 minutes, and the solution was applied to a silicon substrate using a pipette dispenser (DPOP-100-1000, Russia). After the solution has dried, the sample is suitable for AFM studies.

Fig. 2 shows the AFM scan results. The maximum potential difference for one particle is approximately 140 mV. The sign of the potential indicates that the particles are oriented by a metal contact to the surface of the silicon substrate. These data allow an estimate for the particle capacity of the order of 10^{-20} F.

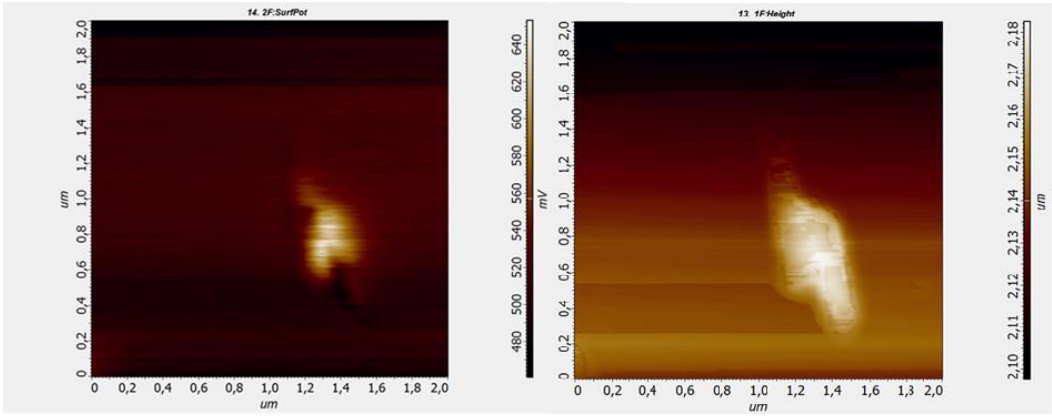

Fig. 2. AFM image of an Ag/Si particle: potential distribution (left) and surface topography (right)

Conclusions

An experimental study of the electrophysical properties of silver nanoparticles has been carried out. The potential distribution over the surface deposited by nanoparticles was measured. The electrical capacity of the nanoparticle was estimated.

References

[1]. Nomoev A.V., Bardahanov S.P. Sintez, stroenie nanochastic metall/poluprovodnik Ag/Si, poluchennyh metodom ispareniya-kondensacii // Pis'ma v ZHurnal tekhnicheskoj fiziki. — 2012. — T. 38. — № 8. — S. 46–53.

[2]. Romanov N.A., Kalashnikov S.V., Tsyrenova M.A., Nomoev A.V. INNOVACIONNYE TEKHNOLOGII V NAUKE I OBRAZOVANII. Proceedings of the 4th international conference. Ulan-Ude, 2015. pp 132-136.

Solid-State [2+2] Photodemirization of *trans*-Cinnamic Acid Derivatives: *trans*-4-(trifluorometyl)cinnamic acid

Chantsalnyam Bariashir[1], Nergui Uranbileg[1], Khongorzul Batchuluun[1], Myagmargerel Bayanmunkh[1], Jargalsaikhan Lkhasuren[1], Tuvjargal Norovsambuu[2,3] and Davaasambuu Jav[2,3]

[1]*Institute of Chemistry and Chemical Technology, Mongolian Academy of Sciences, 13330 Ulaanbaatar, Mongolia*

[2]*Laser research center, National University of Mongolia, 14201 Ulaanbaatar, Mongolia*

[*]*Email: davaasambuu@num.edu.mn*

Abstract: Derivatives of cinnamic acid have been widely studied into photosynthesis, vision, photolithography and photodynamic therapy.[1] Therefore, cinnamic acids have a unique strategy to construct cyclobutanes which are building blocks for a variety of biologically active molecules and natural product. Here we report, the photodimerization of novel highly efficient *trans*-4-(trifluorometyl) cinnamic acid as monomer (Fig. 1) on a molecular level, spectroscopic and photocrystalographic measurements were performed in solid, in solvent as solution and crystal states. Single-crystal X-ray analyse of the intermolecular double bond distances of solid of *trans*-4-(trifluorometyl) cinnamic acid has been exhibited less than 4.2Å and it revealed photodimerization.[2] Single crystals of cinnamic acid obtained from slow diffusion in methanol.

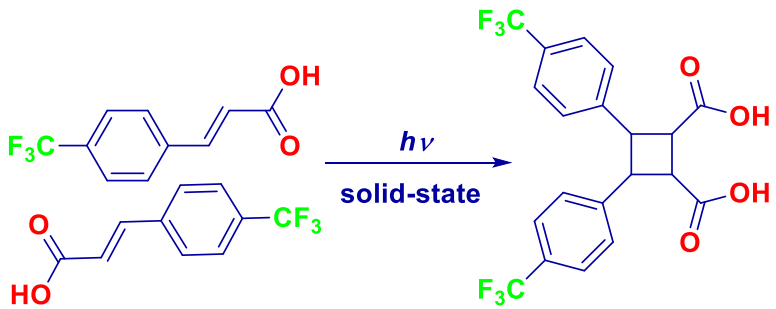

Fig. 1 Photodimerization of *trans*-4-(trifluoromethyl)cinnamic acid

References

[1] (a) V. Ramamurthy, J. Sivaguru, *Chem. Rev.* 2016, 116, 9914–9993; (b) J.B. Benedict, P. Coppens, *J. Phys. Chem. A.* 2009, 113, 3116–3120.

[2] (a) J. Davaasambuu, G. Busse, S. Techert, *J. Phys. Chem. A.* 2006, 110, 3261–3265; (b) J.A.K. Howard, H.A. Sparkes, *Crys. Eng. Comm*. 2008, 10, 502–506.